UCLA School of Engineering and Applied Science

Final Report

1993-94 ADVANCED DESIGN PROGRAM
UNIVERSITY SPACE RESEARCH ASSOCIATION

University of California, Los Angeles

Volume 2: Ion Engine Propelled Earth-Mars Cycler with Nuclear Thermal Propelled Transfer Vehicle

ION ENGINE PROPELLED EARTH-MARS CYCLER WITH NUCLEAR-THERMAL PROPELLED TRANSFER VEHICLE

University of California, Los Angeles
Mechanical, Aerospace and Nuclear Engineering Department
Los Angeles, California

Professor Rudolf X. Meyer
Myles Baker and Joseph Melko - Teaching Assistants

ABSTRACT

The goal of this project was to perform a preliminary design of a long term, reusable transportation system between Earth and Mars which would be capable of providing both artificial gravity and shelter from solar flare radiation. The heart of this system was assumed to be a Cycler spacecraft propelled by an ion propulsion system. The crew transfer vehicle was designed to be propelled by a nuclear-thermal propulsion system. Several Mars transportation system architecturs and their associated space vehicles were designed.

Section 1: Orbital Mechanics

Introduction: Goals

Various types of Cycler orbits to Mars were investigated for this project. Some of the primary goals include: (1) more frequent encounters between Mars and Earth, (2) small delta V angles, at Earth and Mars approach, (3) short length of stay time on the Cycler, and (4) easy predictability of the position of the Cycler. An initial suggestion of placing a Cycler in an orbit that would rotate along with the motion of Mars and Earth was investigated. Other suggestions included: three Cyclers in three different VISIT orbits at various positions between Earth and Mars, and a rotation of one Cycler, in a VISIT orbit, with respect to the inertia frame of the Sun and the planets.

The Up/Down Escalator orbit was ruled out because the delta V was too large for the Taxi to maneuver comfortably. The Cycler would have to travel far out past Mars to be able to encounter the next Mars pass on its down escalator. This long distance would require long periods on the Cycler.

After all the options were investigated, the best choice seemed to be the configuration with three VISIT-like orbits in space at an angle of 130 degrees away from the zero degree VISIT orbit

Options:

Keeping the objectives in perspective, the three approaches were examined. Although the option of placing one Cycler in orbit with a rotation to meet the planets seemed to be optimal, there were drawbacks to this selection. The fuel requirement to rotate the Cycler for it to meet the planets at each window of opportunity was to be about 80% to 85% of the weight of the Cycler. Another drawback to this idea was that the

motion of the Cycler had to be monitored constantly since it was not traveling at a predictable path. For a fifteen-year mission, the cost would become immense. The motion of the Cycler would have to be calculated out in advance in order for the correct encounters to occur. If an error emerged, the problem would propagate to future trips on the Cycler. Above all, there would need to be a constant monitor of the motion and position of the Cycler as well as the planets.

A solution to the predictability problem was to have a Cycler orbit on a preset orbit around the planets. The plane which contained Earth and Mars with the sun as the center was used as the orbit plane. Since the relative position between Earth and Mars repeats every 2.143 years, the Cycler orbit was separated into seven equally angled rotations around the sun. The orbit's major axis was 51.429 degrees away from each other, thus covering the entire range with seven passes. Starting at the Earth, the Cycler would travel in a VISIT 1 orbit to Mars, then, upon returning to Earth's vicinity, the Cycler would perform a delta V with Earth's gravity assist. The delta V would get the Cycler into an orbit that was 51.429 degrees away. This new orbit would have a longer period and different orbital parameters. Table 1 shows the various parameters corresponding to the position of the Cycler and the velocity differences between the planets and the Cycler at the encounter points.

An argument against using this method of approach to Mars was that the Cycler would be rotating for long periods of time without an encounter between either planets. There would be periods of more than ten years before the Cycler met up with Mars and be able to return to Earth. In conjunction to this argument, the fuel requirement for the constant rotation would be on the order of about that of the first proposal. The crew would spend most of its time on the Cycler instead of on Mars as the project proposed. A longer period in space would constitute to a larger supply of food and fuel as well as more recreational activities and living space. With these arguments, it can be deducted that a mission of this magnitude would be practically impossible.

Therefore, a mission consisting of three Cyclers in orbits of 130 degrees away from the zero degree VISIT orbit from Earth to Mars' perihelion was considered to be the most optimal choice. Figure 1 shows the orbit configurations of the three Cyclers. And Table 2 shows the orbital parameters of these Cyclers. As can be seen, the delta V's between the Cycler and Mars are relatively small, translating to a small amount of fuel needed by the Taxi to get to Mars from the Cyclers since Mars is traveling at a faster rate than the Cyclers. Since the small delta V's are accomplished for relatively short amounts of time, the crew should not be too uncomfortable when entering the planets' atmosphere. At encounters with Earth, the delta V's are a bit higher but the difference is not as significant as seen for Earth has a higher gravitational pull.

Table 3 lists the length of each part of the mission. In the eighteen year projection, three complete trips can be predicted. At an initial position where Earth and Mars are 135 degrees apart, the first Taxi should be on the Cycler , travelling to Mars on the zero degree Cycler. It takes 0.442 years to reach Mars. Once on Mars, the crew would stay on the planet for 4.30 years and then return to Earth within 0.669 years. This mission would have a total travel time of 5.41 years. Then the next window of opportunity to go to Mars would be 4.75 years after the initial launch off of the first mission. This time, it would take a total of 3.70 years to reach Mars and the crew would be able to stay on Mars for 2.49 years. The quickest return trip would take 0.543 years. The total mission time would be 6.73 years. The last crew would leave 14.89 years after the initial mission and travel for 0.658 years and stay on Mars for 1.36 years. After which, it would take 0.838 years to return to Earth. This shortest mission would be 2.856 years. Although there may appear to be more opportunities for a crew to travel between Earth and Mars, the planets' position must be taken into consideration. The graph shows the relative position in relation to the sun but upon careful examination, Earth must meet the Cyclers at appropriate intersections and the Taxi must perform small delta V's to make up for the small angle change.

Of course, the time it takes the Taxi to thrust from the planets to the Cycler is considered negligible since it will only take about one day to thrust into a hyperbolic orbit to capture into the planets' gravitational pull. And since a hyperbolic flyby is used, the change in direction for the Taxi to travel is small. With the two orbits in almost parallel positions, the Taxi only needs to make a small adjustment once it leaves the Cycler to meet Mars.

Analysis: The Combination VISIT Orbit

Once the configuration of the orbits was determined, calculations had to be made. Taking into consideration the sphere of influence on both planets, the zero degree VISIT orbit was calculated to have a aphelion distance from the sun, (one of the orbit's focus) of 2.072E+8 km. Since the distance from the sun to Earth is considered to be close to 1 AU after the consideration of the sphere of influence, the perihelion is about 1.4055E+8 km. Knowing these two distances of an ellipse, an eccentricity of 0.19157 can be determined. Having a constant gravitational constant of 1.32712E+11 km^3/sec^2 around the sun, the velocity at any point of the orbit can be determined with the knowledge of the position and semimajor axis. Then the magnitude of the velocity difference can be found by comparing the velocity of the Cycler and Mars. Applying this to the hyperbolic velocity calculation, a true delta V can be found. With this basis, the delta V between Earth and the Cycler can also be determined.

Knowing all the necessary parameters, a position graph can be plotted, as in Fig. 2. Where the paths of the Cycler and the planets meet are the points of connection between the two bodies. Theoretically, there are more points of connection but the position of the planets must be taken into consideration. Examining the graph, there are three complete missions that are possible. Table 3 lists the duration of each leg.

With all the parameters available, the delta V's of the Taxi maneuvers can be calculated. As shown in Table 2, the delta V's for each Cycler as it meets Mars is between 5.27 and 6.32. With Earth, the delta V's are larger: between 9.49 and 10.46. These delta V's have taken the hyperbolic capture into consideration since the mission will consist of capture into the planets' atmosphere by means of a hyperbolic fly-by. The Cyclers will meet Mars' orbit before Mars arrives at that position and launch the Taxi. At that point, the Taxi performs a delta V thrust into Mars capture orbit. Figure 3 shows this maneuver. The same principle applies to the capture into Earth.

The thrust required to accomplish these maneuvers would be less than the engines are able to perform therefore, the maneuvers are possible. The largest thrust needed on the Taxi is 5.639E+5N but the engines are able to perform thrusts of up to 6.98E+5N.

From Earth's Low Earth Orbit, LEO, the Cycler would need to spiral out to its final zero thrust orbit by nearly circular orbits around Earth. For this spiral maneuver, the Cycler would need 98.4N of thrust and the engines are able to supply a thrust of 150N, therefore the mission is saved. Figure 4 shows the Cycler's spiral maneuver.

Having calculated the parameters for the first Cycler orbit, the other two Cycler orbits' parameters are calculated using the same equations (given in the appendix). The number two Cycler is rotated by 130 degrees counter-clockwise, while the number three Cycler is rotated 230 degrees clockwise. Since Mars has an elliptical orbit, the aphelion and the semi-major axis are different than that of the VISIT orbit at zero degrees. Taking that into consideration, the parameters for these two orbits are also given in Table 2.

Conclusion:

With this configuration of orbits, optimal conditions are accomplished. With three Cyclers, the number of complete missions increase and the length of the trips are shortened. Since the orbits meet nearly tangentially to the planets' orbits, the amount of fuel required to perform the delta V's are lowered and the change of angle between the two orbits are lessened. These circumstances meet the criteria of the project. For an eighteen year projection of the mission, three trips can be obtained, thus justifying the cost and time of the entire project.

References:

1. "Project Minerva : A Low Cost Manned Mars Mission Based on Indigenous propellant Production"; Final Report, NASA, Washington University, Seattle, June 1992.
2. "Project WISH: The Emerald City, Phase 2", NASA, Ohio State University, Columbus, June 1991.
3. "Optimization of Double Swingbys", NASA, Akademiya Nauk SSSR, Moscow. Inst. Kosmicheskikh Issledovanii, December, 1991.
4. French, James R. and Griffin, Michael D., Space Vehicle Design. American Institute of Aeronautics and Astronautics, Washington DC, 1991.

Appendix:

To calculate the orbital parameters, simple orbital mechanics equations were used. Having the equation of an ellipse:

$$r = \frac{a(1-e^2)}{1+e\cos v}$$

the velocity can be determined by

$$v = \sqrt{\mu\left(\frac{2}{r} - \frac{1}{a}\right)} \ .$$

Calculating the sphere of influence for both planets by using:

$$r \cong R(m/M)^{\frac{2}{5}}$$

and using the Earth's distance from the sun, 1AU, minus the sphere of influence to be the perihelion of the Cycler orbit, the eccentricity can be determined. Since the perihelion r_p and aphelion r_a for the orbits are known, the eccentricity is:

$$e = \frac{r_a - r_p}{r_a + r_p}$$

and the semimajor axis is:

$$a = \frac{r_a + r_p}{2}.$$

Applying the same velocity equation as above, the velocity of the Cycler is calculated.

Then using the equations for a hyperbolic trajectory, the velocity of the Cycler as it passes the planets is:

$$v_p = \sqrt{\left(v_\infty^2 + \frac{2\mu}{r_p}\right)} - \sqrt{\frac{\mu}{r_p}}.$$

To graph the positions of the planets and the Cyclers the radial distance of an ellipse is used. The positions:

$$r = a(1-e\cos E)$$

where

$$\cos E = \frac{e + \cos \nu}{1 + e \cos \nu} \quad .$$

The time for the objects to reach a specific position is calculated as:

$$t = \frac{E - e \sin E}{n}$$

where n is defined to be the mean anomaly of the orbit. And is calculated by

$$n = \sqrt{\frac{\mu}{a^3}} \quad .$$

To calculate for the thrust,

$$T = \frac{m_o g_o Isp}{t_1 - t_0} \left(1 - \exp \left(\frac{-\sqrt{\mu \left(\frac{1}{r_0} - \frac{1}{r_1} \right)}}{g_o Isp} \right) \right)$$

where:

m = initial mass of the vehicle

g = standard gravity

Isp = specific impulse

μ = gravitational parameter.

r = radius

t = time of travel

MARS											
H=r*v	5.476E+09			0	1	2	3	4	5	6	7
nu	1.327E+11		angle	0	51.42857	102.85714	154.28571	205.71429	257.14286	308.57143	360.00000
			angle rad	0	0.89760	1.79520	2.69279	3.59039	4.48799	5.38559	6.28319
p	2.259E+08		**r vector**	2.07E+08	2.13E+08	2.31E+08	2.47E+08	2.47E+08	2.31E+08	2.13E+08	2.07E+08
e	0.09338		r scaler	2.07E+08	2.13E+08	2.31E+08	2.47E+08	2.47E+08	2.31E+08	2.13E+08	2.07E+08
			a	2.28E+08	2.28E+08	2.28E+08	2.28E+08	2.28E+08	2.28E+08	2.28E+08	2.28E+08
			v vector	2.65E+01	2.57E+01	2.38E+01	2.22E+01	2.22E+01	2.38E+01	2.57E+01	2.65E+01
			v vector	2.65E+01	2.57E+01	2.38E+01	2.22E+01	2.22E+01	2.38E+01	2.57E+01	2.65E+01
CYCLER			r-a	2.07E+08	2.13E+08	2.31E+08	2.47E+08	2.47E+08	2.31E+08	2.13E+08	2.07E+08
			r-p	1.50E+08	1.50E+08	1.50E+08	1.50E+08	1.50E+08	1.50E+08	1.50E+08	1.50E+08
			e	1.60E-01	1.76E-01	2.13E-01	2.45E-01	2.45E-01	2.13E-01	1.76E-01	1.60E-01
			a	1.78E+08	1.82E+08	1.90E+08	1.98E+08	1.98E+08	1.90E+08	1.82E+08	1.78E+08
			b	1.76E+08	1.79E+08	1.86E+08	1.92E+08	1.92E+08	1.86E+08	1.79E+08	1.76E+08
			period (s)	4.10E+07	4.22E+07	4.52E+07	4.81E+07	4.81E+07	4.52E+07	4.22E+07	4.10E+07
			v	2.32E+01	2.26E+01	2.13E+01	2.02E+01	2.02E+01	2.13E+01	2.26E+01	2.32E+01
			delta v	-3.273960	-3.076316	-2.562880	-2.064943	-2.064943	-2.562880	-3.076316	-3.273960

Table 1: Seven Orbit Rotation

Table 2:	Orbital Parameters				
	Mars		**0**	**1**	**2**
		ANGLE	0	130	230
		ANGLE RAD	0.0000	2.2689	4.0143
		R POSITION	2.0663E+08	2.4036E+08	2.4036E+08
		a	2.2792E+08	2.2792E+08	2.2792E+08
		VELOCITY	26.4995	22.8474	22.8474
	Cycler	PERIOD (YR)	1.253	1.439	1.439
		TIME IN SEC	3.9536E+07	4.5425E+07	4.5425E+07
		R a	2.0716E+08	2.4088E+08	2.4088E+08
		R p	1.4055E+08	1.4055E+08	1.4055E+08
		e	1.9157E-01	2.6304E-01	2.6304E-01
		a	1.7385E+08	1.9071E+08	1.9071E+08
		n	1.5892E-07	1.3832E-07	1.3832E-07
		VELOCITY	22.7575	20.1500	20.1500
		DELTA V	6.3152	5.2707	5.2707
	Earth	vel of cycler	33.5428	34.5341	34.5341
		vel of earth	29.7844		
	Hyperbolic	vel peri	35.9883	33.3028	33.3028
		delta v	9.4889	10.4554	10.4554
sphere of influence		mars	5.2305E+05		
		earth	9.2459E+05		

Table 3:	Length of Legs of Mission				
		Trip	**From Earth to Mars**	**Stay on Mars**	**From Mars to Earth**
		1	0.422 yrs	4.30 yrs	0.669 yrs
		2	3.70 yrs	2.49 yrs	0.543 yrs
		3	0.658 yrs	1.36 yrs	0.838 yrs

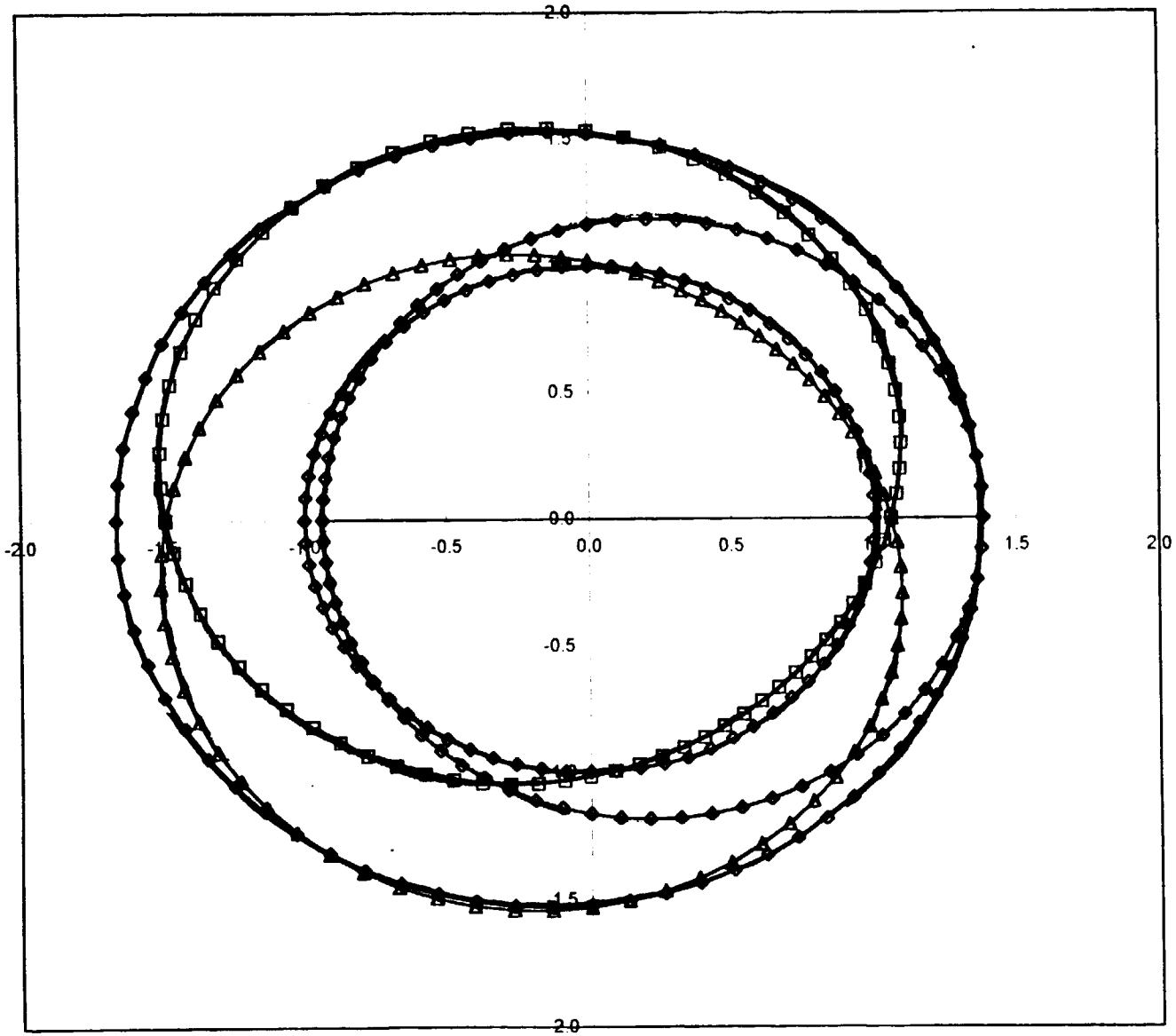

FIG. 1 ORBITS OF CYCLERS WITH PLANETS

Section 2: Cycler Design

In order for our proposed cycler project to run smoothly, there are a few projects that are prerequisites to the launching of our cycler. First, there must be an Earth orbiting space station. This is necessary as a base of operations for cycler construction and it would also be the rendezvous spot for the taxi between the cycler and Earth. It is assumed that the outbound astronauts would be transferred to the space station from a conventional shuttle and would be taken from the space station to the cycler ship by way of the taxi. Upon return to Earth, the astronauts would be transferred to the space station by the taxi and would return to Earth inside a shuttle. The second critical project is an established base on the surface of Mars. Our envisioned cycler project assumes that there have been previous manned missions to Mars which have created habitats on the surface of Mars as well as a landing / launch pad for the cycler's taxi. Third, a hydrogen electrolysis plant on Phobos is needed to produce the hydrogen that is used by the taxi. The amount of fuel required by the taxi is so large that our proposed taxi can only hold enough fuel to get to Mars and needs to be refueled to get back to the cycler. This creates our last necessity, a fuel ship to transfer fuel from the electrolysis plant to the Mars orbiting first stage of the taxi.

The Mars Cycler is designed to transport sixteen crew members to Mars. The overall configuration is shown in perspective in Fig. 2-1. Figure 2-2 shows the front view of the cycler. The sixteen crew members are divided into two groups of eight and each group has its own crew module as shown in the figure. These crew modules are placed at a distance at opposite sides of the central cycler. When spinning, the cycler provides artificial gravity in the crew modules equal to 3/10 the force of gravity on Earth. The rate of rotation as well as the distance from each crew module to the central axis were computed as follows:

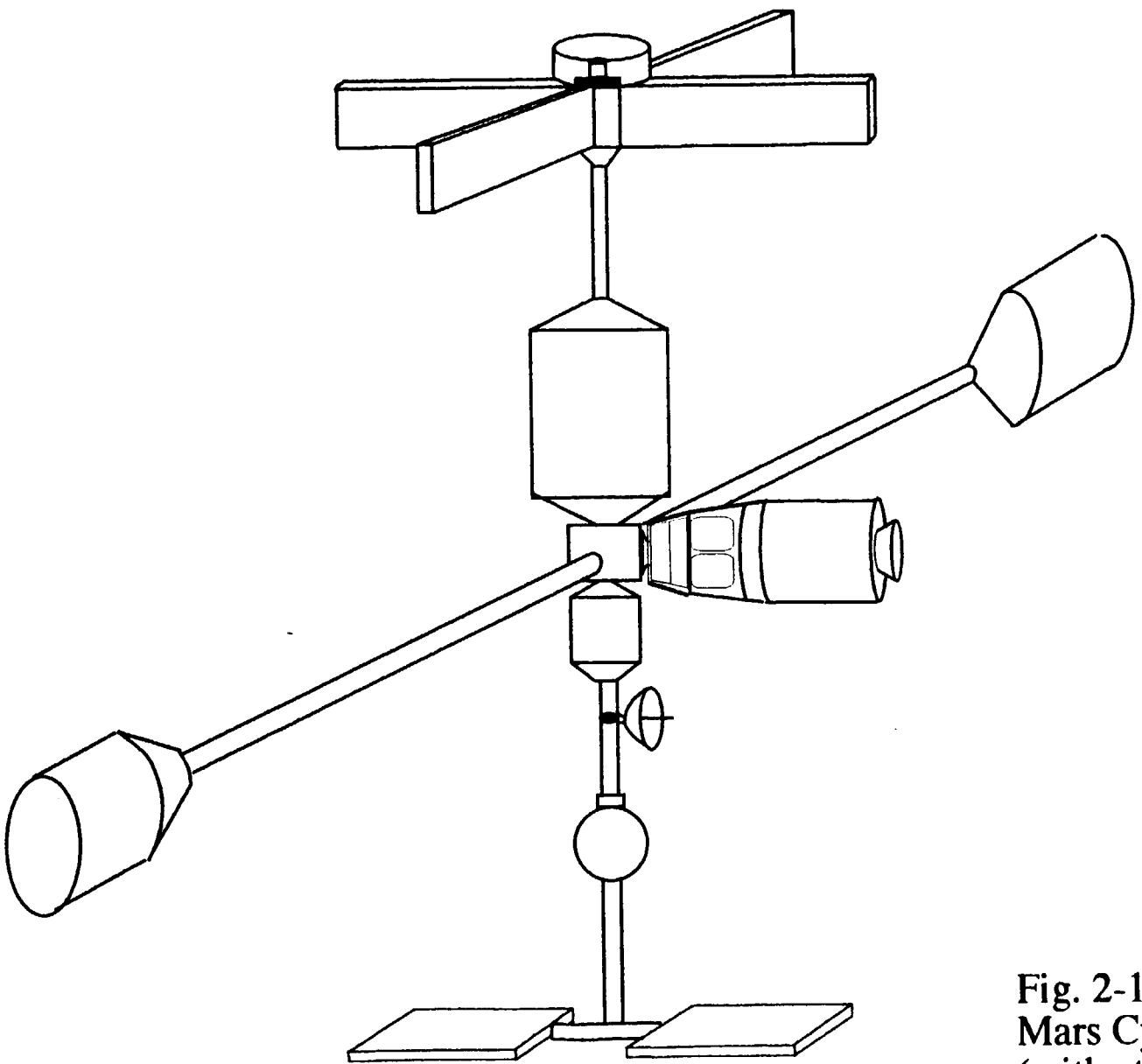

Fig. 2-1
Mars Cycler
(with attached taxi)
Group 1
R.C.

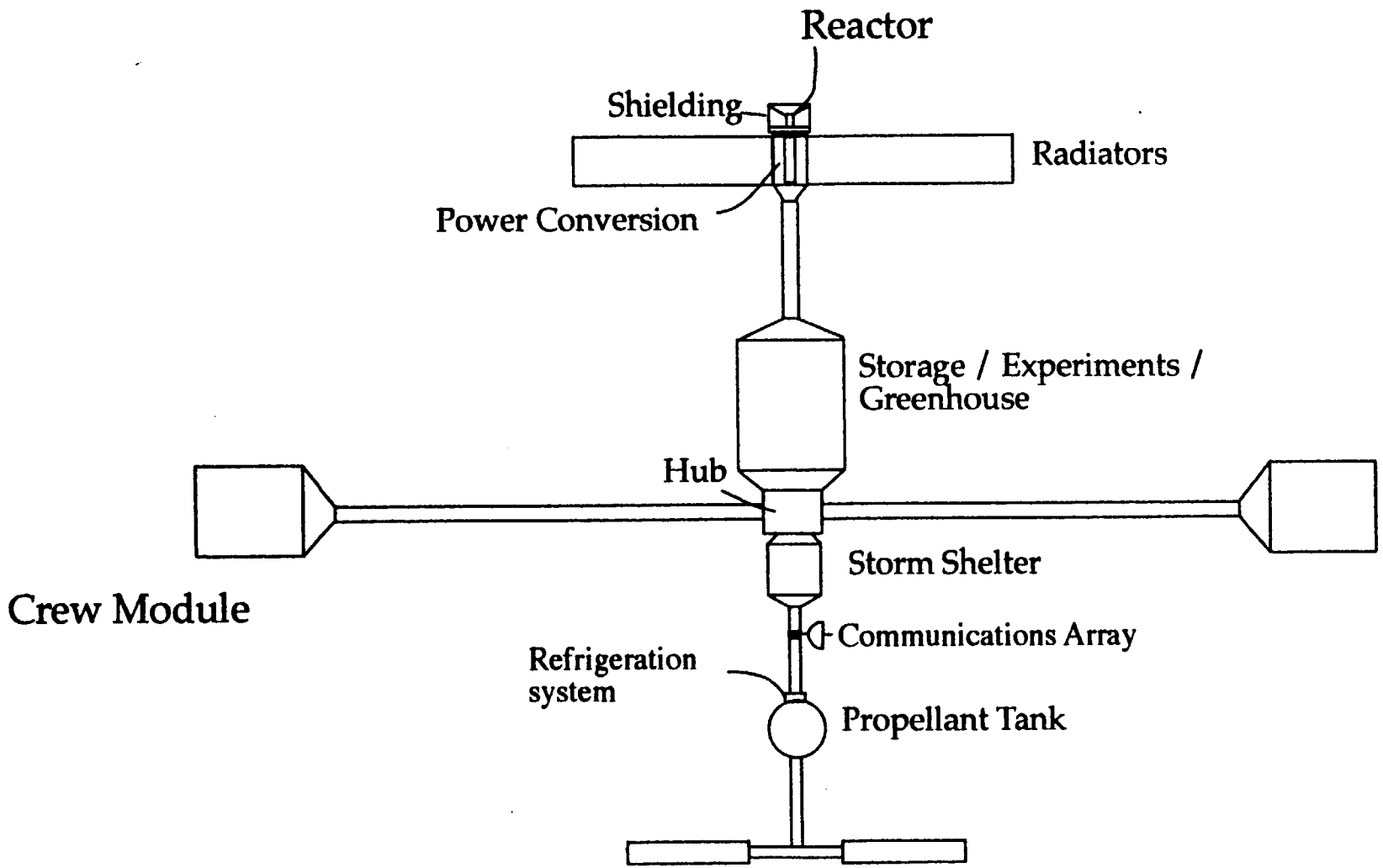

Fig. 2-2
Group 1
Mars Cycler
Richard Cribbs

$$a = v^2 / r$$

$$v = \omega r \Rightarrow a = \omega^2 r$$

The coriolis acceleration < 10% of artificial gravity

$$v_r = 0.50 m/s$$

$$coriolis = 2\omega v_r = \omega$$

$$\Rightarrow \omega \leq 0.2943 rad/s$$

$$r = \frac{a}{\omega^2} \Rightarrow \omega = 2.32 rpm$$

$$r = 50m$$

$$a = 0.30g$$

Artificial gravity is deemed necessary because of the long times spent traveling in the cycler spacecraft. NASA studies have shown the detrimental effects of prolonged weightlessness including bone decalcification and muscle atrophy. It was assumed that an artificial gravity of 0.3 g would be adequate so that the astronauts would be able to function upon arrival at Mars.

The bulk of the Cycler's mass is positioned on the central axis. This creates the smallest moment of inertia which in turn allows for the least amount of propellant required to spin and despin the Cycler. The Cycler must be despun for docking and releasing the taxi. Small reaction control jets are positioned at the ends of each crew module. When fired, these jets produce a couple that spins or despins the Cycler. The distance between the thrusters (108 m) combined with the small rotation rates needed (2.38 rpm) makes these small reaction control jets feasible as a means for spinning or despinning the Cycler.

Connecting each crew module to the hub are permanent tunnels. Originally collapsible tunnels were envisioned that would stay out of the way for most of the journey but permanent tunnels seemed more practical. The permanent tunnels are less likely to suffer failure as the are not moving pieces. The amount of travel between the crew modules and the greenhouse / storage module would have made waiting for the extension

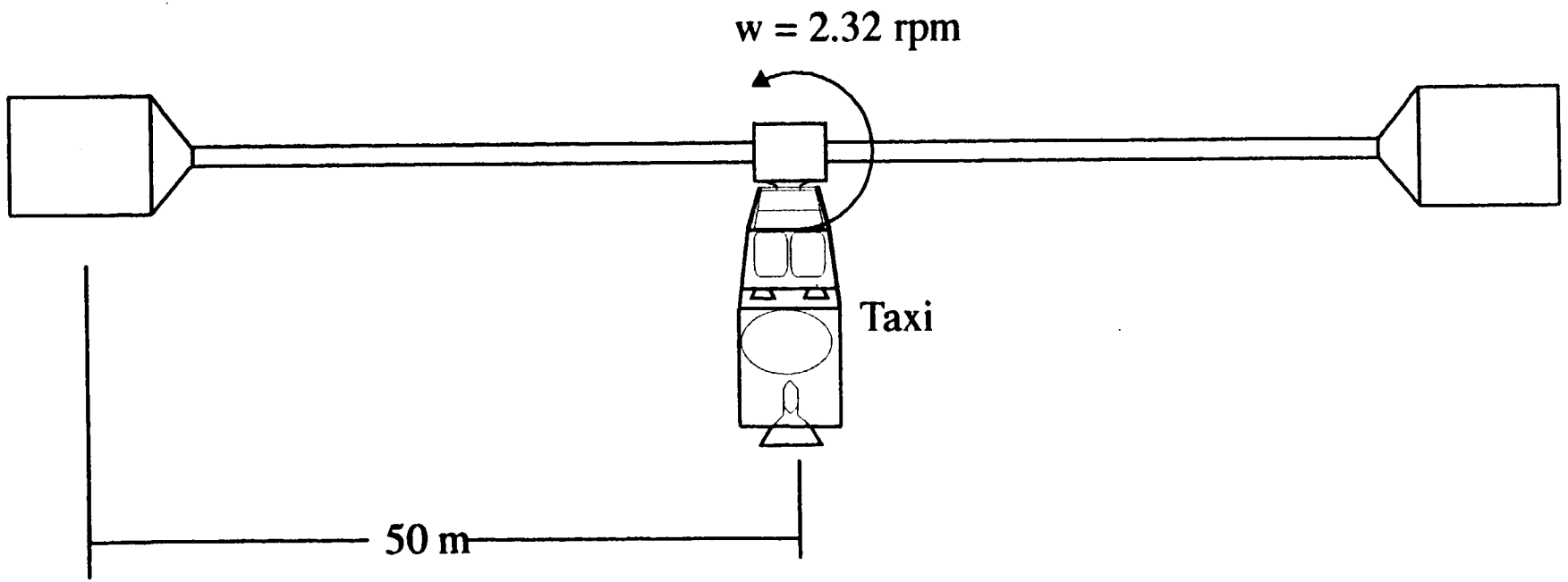

Fig. 2-3
Top View
Mars Cycler
Group 1
RC.

of the collapsible tunnel unbearable. Micro-meteorites also posed a serious threat to the collapsible tunnels. The penalty of extra weight is acceptable for the trade off of greater ease of use.

The tunnels join in the center of the spacecraft at the hub. The hub is the central joint of the cycler and is where the taxi docks with cycler as shown in Fig. 2-3. The nose of the taxi is actually a retractable shroud that protects the docking mechanism of the taxi. When nearing the cycler, this shroud is collapsed exposing the docking tunnel and allows the taxi to couple with the Cycler.

Adjacent to the hub is the storm shelter. Solar periodic events create huge radiation levels. Without a storm shelter, the astronauts would have inadequate protection to survive these events unscathed. The storm shelter was designed to accommodate all sixteen crew members and to provide protection for the astronauts such that each astronaut receives no more than 50 rems. The solar periodic events are normally short lived so the astronauts' accommodations are quite sparse. As shown in Fig. 2-4, the storm shelter is two tiered. The astronauts are seated in semi-reclined chairs so that they can either sleep or do work. The height of each level does not allow for the astronauts to stand so they are assumed to be seated for the duration of the storm. Aluminum shielding was chosen over water and liquid hydrogen shielding mainly due to the ease of construction and maintenance. With no moving fluid, mechanical failure of the shielding will not occur. The thickness of the storm shelter was sized using information from NASA report 1257 and the data is listed in figure 2-5.

Storm Shelter

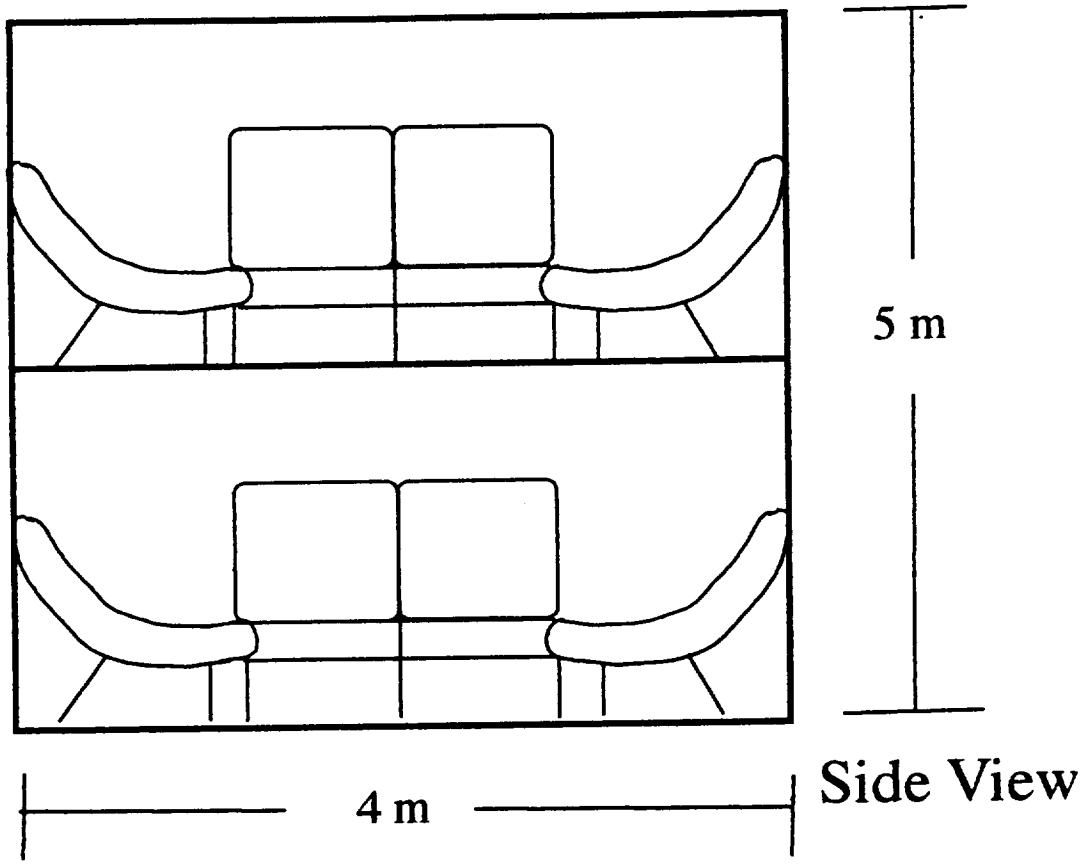

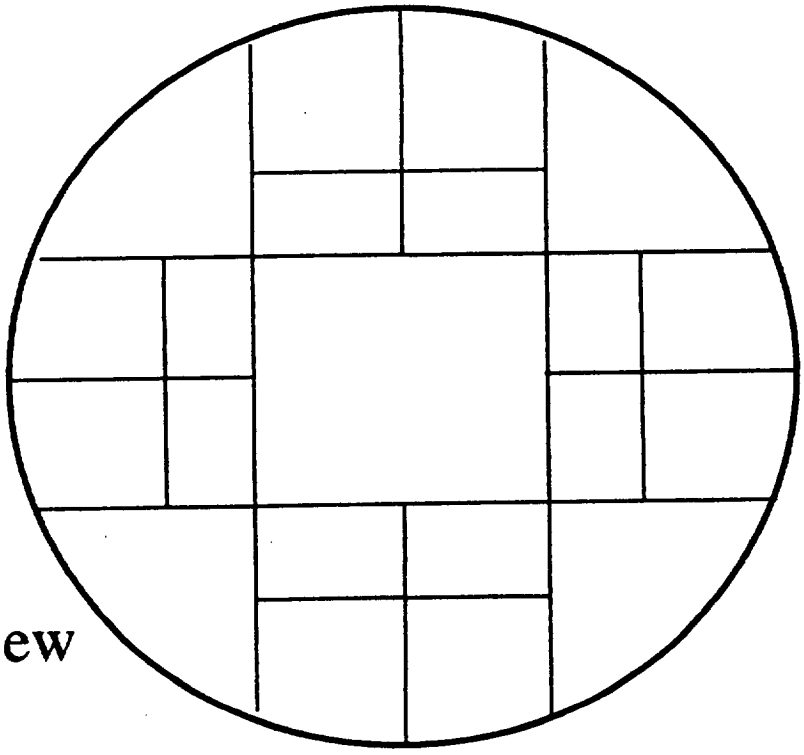

Fig. 2-4
Mars Cycler
Group 1
R. C.

Fig. 2-5

Dose equivalents for large Solar Periodic Events

Tables 11.25 and 11.27 (NASA RP. 1257, Transport Methods and Interaction for Space Radiation)

	Aluminum shield thickness, g/sq. cm.	Dose equivalent (Sv) 8/72 SPE	Dose equivalent (Sv) 8/72 and 2/56 SPEs combined
Skin	2	11.30	14.2
	20	0.18	0.43
Ocular Lens	2	9.09	11.3
	20	0.17	0.43
BFO	2	1.24	1.64
	20	0.07	0.31

This table compares radiation levels in 3 organs using 2 or 20 grams per square centimeter aluminum. The August 1972 solar periodic event was the largest ever recorded while the February 1956 event contained the most harmful spectrum to date. The final column shows the expected radiation level of a solar event with the duration and intensity of the 1972 event combined with the harmful spectrum of the 1956 event. From this table it is seen that the highest levels of radiation occur in the skin while the blood fluid organs (BFO's) suffer the least amount of radiation. Using 20 grams per square centimeter aluminum provides protection so that 43 rems is the largest dose an astronaut could expect to see. Therefore, 20 grams per square centimeter was chosen. This is equivalent to 7.4

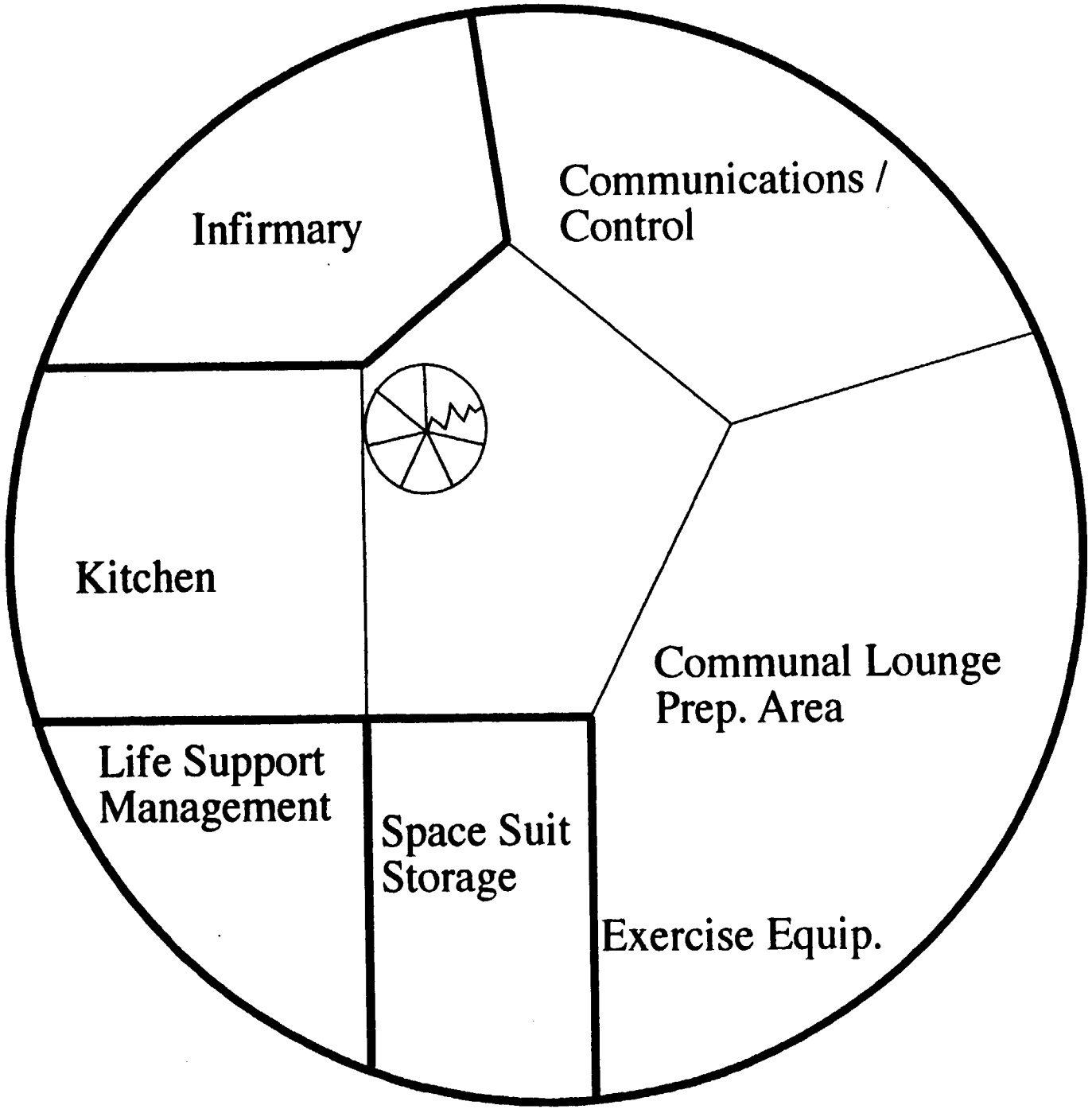

Fig. 2-6

Mars Cycler
Second Level

RC

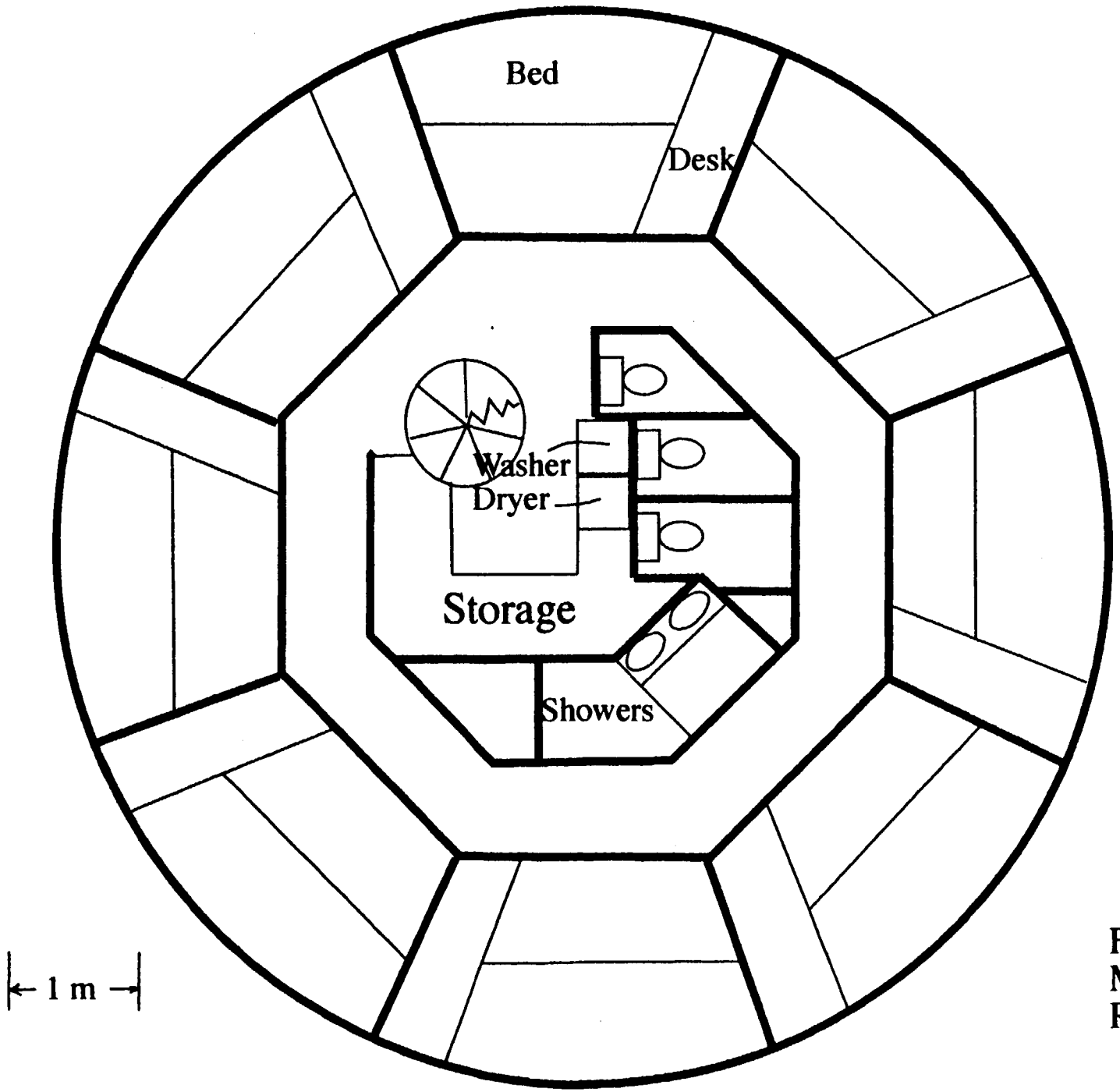

Fig. 2-7
Mars Cycler
Residential Floorplan

RC

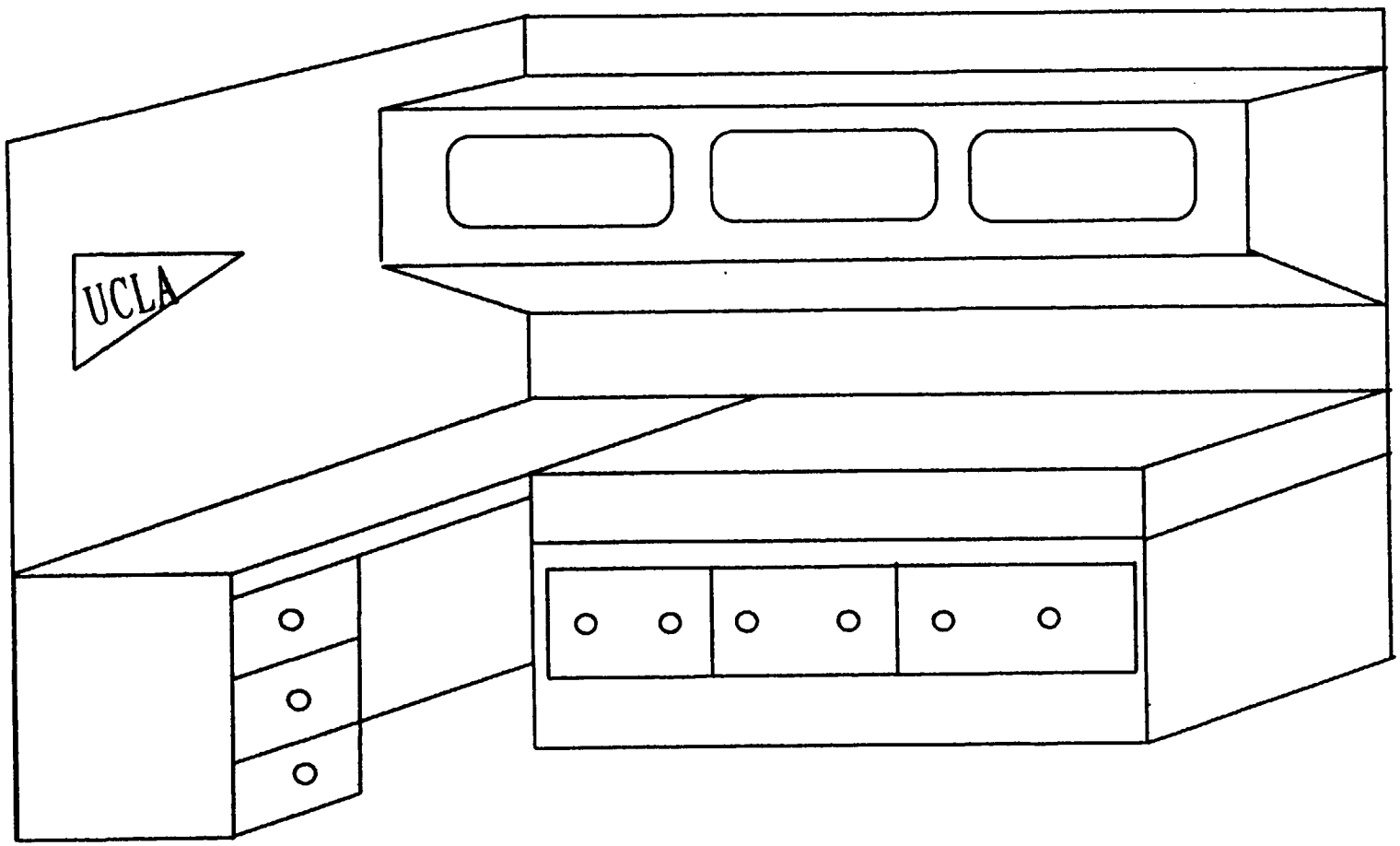

Typical Crew Quarter

Fig. 2-8
Mars Cycler
Group 1

RC

cm thick aluminum. As designed, the storm shelter requires 760,000 square cm of aluminum. This equates to 15,000 kg!

Each crew module is divided into two levels with the upper level as the communal level while the lower level is the residential level. (See figures 2-6 and 2-7) Included on the communal level are the exercise area and the infirmary. At least two doctors per crew are part of the mission and with such long missions, a dedicated sickbay is necessary. Each crew member receives his/her own room. Each room is 2 meters by 3 meters and contain a bed and a desk. The astronauts can retire to the privacy of their own rooms where the decor can be customized to satisfy the individual astronaut. A typical crew quarter is shown in figure 2-8. This room just shows the basic configuration without any personalized effects. Storage for the crews personal belongings is provided both in each crew quarter as well as in large storage areas in the center of the residential level.

The greenhouse / storage module above the hub as shown in figure 2-2 contains space for zero gravity experimentation, food storage and life support reclamation systems. The water in the cycler is fully recycled as illustrated in figure 2-9. Potable water is stored in 4 tanks that distribute the water to the various areas on the cycler. Waste water from the toilets is pretreated with waste products removed before joining with the gray water from sinks and showers in the hygiene water reclamation system. The hygiene water reclamation system contains various filtration schemes. First comes a chemical treatment and then the water passes through a charcoal filtering medium. Wet/dry trickle filters provide biological filtration using aerobic bacteria to breakdown harmful nitrates and nitrites. Venturi protein skimmers are utilized to bubble out proteins. Waldman's dark green lettuce (Lactuca Stavia L. Var. Crispa L.) is used as both a water purifier and a source of food. Studies were done on this lettuce by Ricardo Jacquez and Michael Montoya which showed the feasibility of the lettuce as a food source that could also clean water (See Proceedings of Space '94, Vol. 2). The water would then be run through a UV

Water Reclamation System

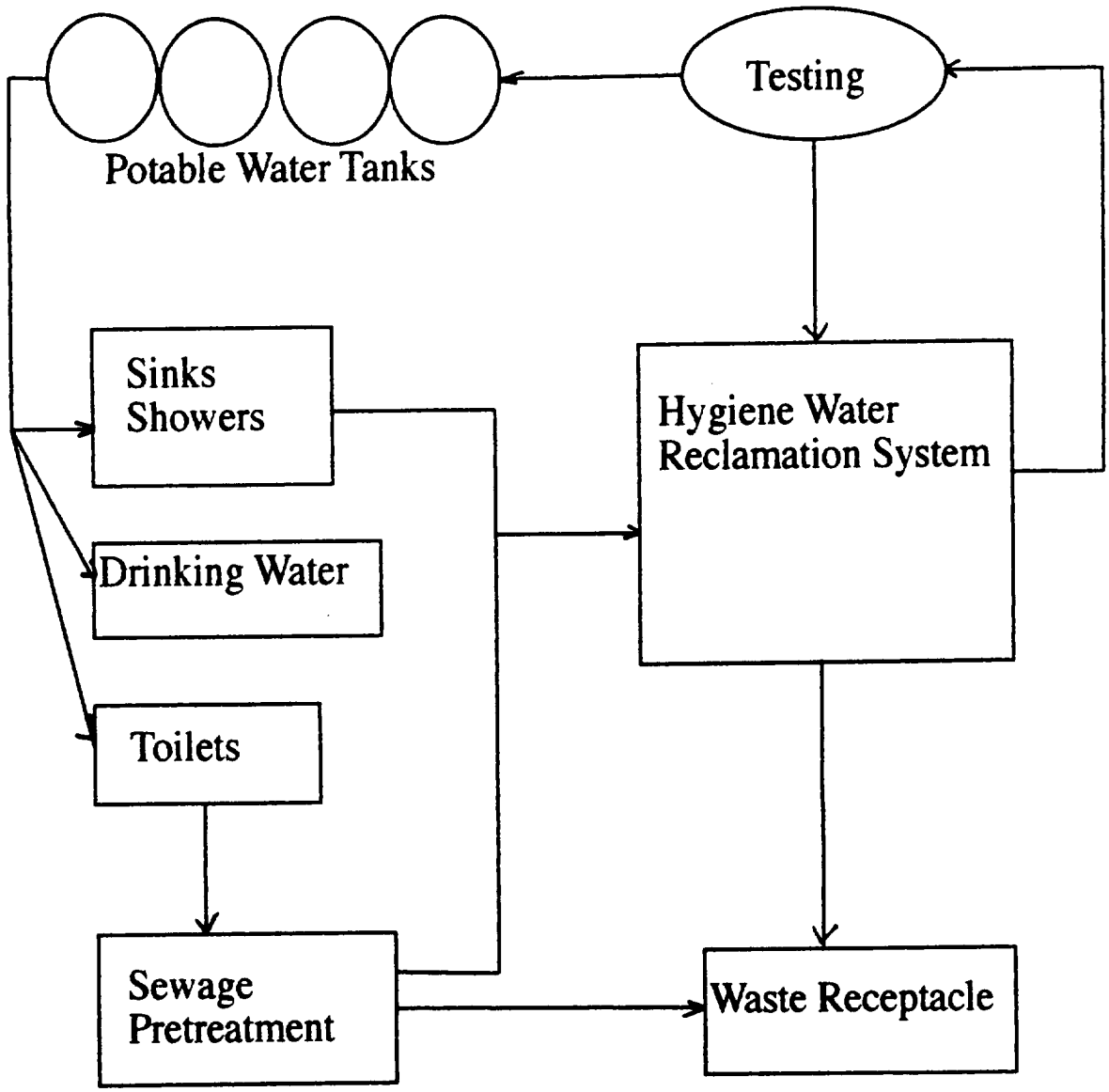

Figure 2-9

RC

sterilizer to kill any living particles and would be run through an algae scrubber and a reverse osmosis filter. Following this, the water would be tested and either be rejected and sent back to the hygiene water reclamation system or have nutrients replaced and returned to the potable water tanks. Along with the water reclamation system will be a green house where some of the astronauts food will be grown under a combination of fluorescent, actinic and halogen bulbs to recreate the spectrum of the sun. This greenhouse would aid the oxygen reclamation system.

Communication to and from the cycler is accomplished using the communication array which is located on the cycler's main axis and is despun. Rings and brushes on the coupling are used to transfer information form the spinning cycler to the despun communications array.

The ion propulsion engines are fueled by argon and there are 60 of the 165 kg, .85 meter diameter engines. Each engine produces 4.4 N of thrust. The high specific impulse of the ion engines allows for very efficient fuel usage and our cycler only requires one 1.5 m radius tank. This provides for a volume of 14.14 cubic meters of argon @ 87 K and 1 atm. As the argon is used, an inflatable bladder within the propellant tank fills with hydrogen from a small external tank. The pressure inside the tank stays constant at 1 atmosphere so there is no problem with the argon expanding and sputtering the ion engines. Also, since both argon and helium are inert, no foreseeable problems exist concerning the degradation of the inflatable bladder. The propellant tank contains 1/3 inch thick 2024 aluminum. The stresses in the tank walls were estimated by cutting the spherical tank in half and analyzing the forces on the half sphere. The overall force caused by the pressure of 1 atm was calculated to be 153218.8 lbs. This equates to a tensile stress of 1283 psi.

We chose a reactor to provide 10MWe power. Combined with a Stirling cycle power converter that has a thermal efficiency of 0.254, this sizes our reactor that generates

40 MWth. It was assumed that in the future, reactors providing 500 kWe/kg would be developed (some books showed up to 3000 kWe/kg as future goals). This is a far cry from the current Snap-100 reactors. To radiate the excess heat, radiators operating at 1000K were sized to need 1000 square meters of surface area. Approximate power plant masses are shown in Fig. 2-11 along with mass estimations for the rest of the cycler. This figure shows a cycler dry weight of 112,000 kg and an overall weight of 130,000 kg fully fueled.

The taxi as shown in Fig. 2-10 is comprised of two stages. The upper stage, which includes the command module and room for all 16 astronauts only separates from the first stage for mars landing. The upper stage is based on McDonnell Douglas' DC-X (the Delta Clipper) which allows for vertical take-off and landing. This upper stage is propelled by conventional liquid chemical rockets. The whole reason behind this separating stage is to prevent contamination of the Martian surface by the radiation from the nuclear thermal reactors that comprise the two engines of the first stage. In this way, areas on Mars are not turned uninhabitable and extra precautions do not need to be taken by the disembarking astronauts to avoid radiation. In this scheme, the nuclear propulsion provides the propulsion to get from the cycler to a Mars orbit. There are two nuclear engines each with a nozzle diameter of 2.5 meters. Once in the Mars orbit, the stages separate and the DC-X lands on Mars while the first stage retains its orbit about Mars. When departing Mars, the DC-X recouples with the recently refueled first stage in the Mars orbit (via the refueling vessel mentioned in the opening paragraph of the design section) and the taxi returns to the cycler. Assuming an overall mass of the taxi equal to 30,000 kg, 22,000 kg is needed as propellant leaving a dry weight of the taxi of approximately 8,000 kg. This means that the taxi is almost a flying fuel tank. The 22,000 kg of liquid hydrogen takes up 310 cubic meters. The estimation of 8,000 kg for the dry mass of the taxi could prove to be overly optimistic in which case a heavier taxi would need to be evaluated.

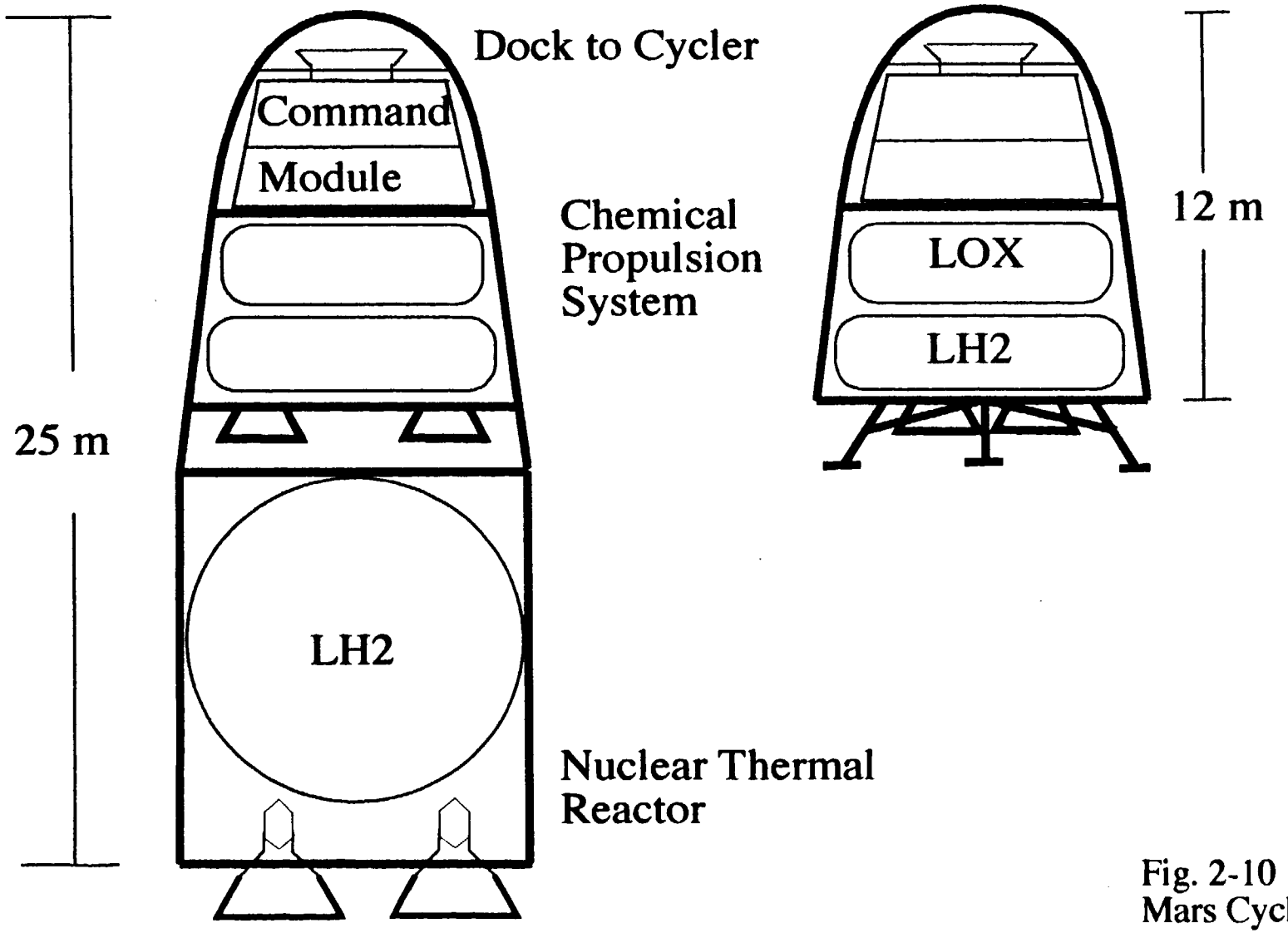

Fig. 2-10
Mars Cycler
Taxi
Group 1

RC

Fig. 2-11
Cycler Mass Estimations

			Mass (kg)
Structure			
	Storm Shelter		15000
	Crew Modules	2@7800 =	15600
	Hub		1500
	Truss		1000
	Tunnels		7500
	Storage/Greenhouse		12500
	Propelant Tank		650
	Refrigeration Cycle		31
Reactor			
	Reactor and Controls		30
	Radiator		2000
	Shielding		1500
	Thermal Converter		250
	Insulation		300
	Power Conversion		120
	Interface Structure		300
Propulsion			
	Argon	13 m3@1390 kg/m3	18000
	Ion Engines	60@165kg	9900
Crew/ Equipment/Supplies			
			43819
		Total =	130000 kg

R.C.

References

"Engineering and Configurations of Space Stations and Platforms:, NASA, Noyes Publications, 1985.

French and Griffin, Space Vehicle Design, AIAA, 1990

Galloway, Engineering, Construction, and Operations in Space IV, ASCE, 1994.

Halliday and Resnick, Physics, 3rd Ed., Wiley and Sons, 1986.

Kaplan, Modern Spacecraft Dynamics and Control, Wiley and Sons, 1976.

Lovelock and Allaby, The Greening of Mars, St. Martin's/Marek, 1984

NASA, Living and Working in Space - A History of Skylab, NASA,1983.

NRC, Space Station Engineering Design Issues, National Acadamy Press, 1989.

O'Leary, Mars 1999, Stackpole Books, 1987

Oberg, Spacefarers of the 80's and 90's, Columbia University Press, 1985.

"Transport Methods and interactions for Space Radiations, NASA Ref. Pub 1257, 1991.

Woodcock, Space Stations and Platforms, Orbit Book Co., 1986

Section 3: Propulsion

Introduction

There are many types of propulsion systems available today and in the future that can be considered for this mission to Mars. We settled on a high efficiency ion-propulsion system. Ion propulsion is a highly efficient method of propulsion, but it does pose the problem of an extremely low thrust. As discussed in the Design section, the mass of the cycler is 130,000 Kg. However, we do have the luxury of taking our time in putting the cyclers into their respective orbits.

The taxi used to go between the planets, space stations, and the cyclers provided a more difficult problem for propulsion. Normal chemical rockets lack the efficiency needed to make the long trips and ion propulsion was just not fast enough. Therefore, it was decided to use a hydrogen nuclear-thermal propulsion system. This provides a reasonable fuel efficiency and a very high thrust.

Ion-Propulsion

The most successful electrostatic thrusters use propellant atoms ionized by electron bombardment. The electrons are emitted from a cathode surface and gain energy from the potential difference between the cathode and anode surfaces in a bombardment ionization chamber.

Figure 4-1 shows a schematic diagram of a generic ion thruster. On the way to the anode (chamber wall), the electrons accelerate and bombard neutral propellant atoms entering from the left-hand side of the chamber. A positive ion is produced when an electron-atom collision is successful. The positive ions then pass through the screen and are accelerated by the screen-accelerator potential difference, producing high-velocity exhaust beam. A neutralizer beam of electrons (not shone) must be emitted from the chamber to maintain a zero net charge for the vehicle. Failure to do this will result in the

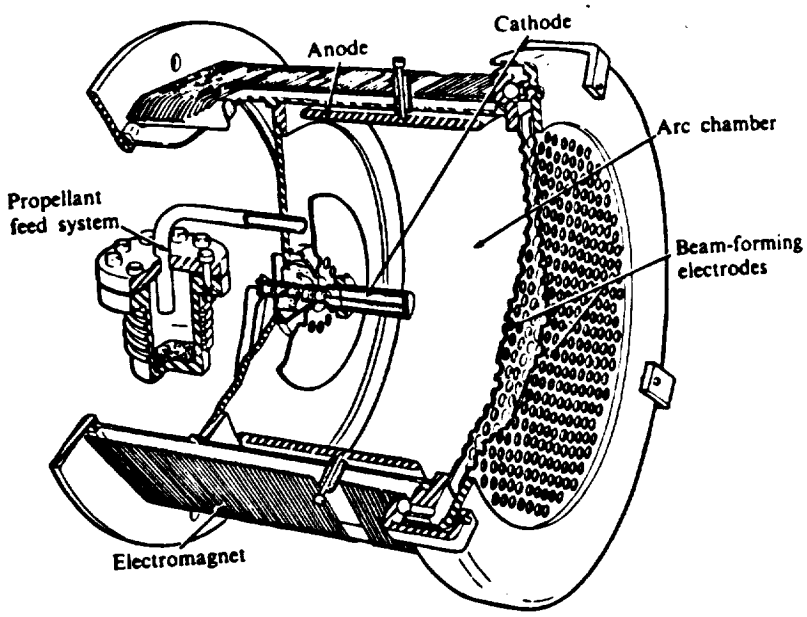

Figure 4-1. Diagram of an ion engine

exiting plasma beam to return to the positively charged vehicle, resulting in a zero net force and damaging the hull and other instruments on the exterior of the vehicle. To increase the chance of a collision, an axial magnetic field is employed forcing the electrons to follow a longer spiral path as opposed to a straight line between the anode and cathode.

Fuels considered for this thruster were mercury, xenon, argon, and potassium. Mercury has the nicest of all the fuels because of it has the highest potential thruster efficiency and needs minimum tankage mass; however, because of its toxicity, it should not be used in near earth maneuvers. Potassium also had good potential, but it required a boiler since its normal form is a solid; this posed problems of having a steady flow of fuel in a consistent form. Both xenon and argon are clean and easily used as a fuel. Xenon tends to be relatively expensive, but it can be stored noncryogenically. Argon does require cryogenic storage, but is less expensive and more plentifully available than xenon.

Instead of designing the entire thruster, we used a similarly designed engine that runs on potassium. The exit diameter is 0.85 meters and has a specific impulse of 10,000 seconds. For an optimized ion thruster, argon has an efficiency of about 80% at 10,000 Isp. Xenon has about a 90% efficiency, so the tradeoff is appreciable, but not enough to

justify the expense of xenon. The potential difference required for argon across the engine is about 2007.32 volts and produces a 7.6 megawatt beam. This is possible because the nuclear power source for the cycler produces about 10 megawatts of power. For safety and to leave power for other systems during the establishment of the final orbit, only 9.50 megawatts is used for propulsion. Each engine produces about 4.4 Newton's of force and expends 1.579E-3 kilograms of argon per second; so for a 130,000 kilogram cycler, 35 engines was deemed a reasonable number. Ion engines, though, have a tendency of failure in the acceleration screen due to damage from ions that deviate from the ion stream. Thus, a 70% safety margin is added to bring the total number of engines to 60; however, only 35 engines would be used at any one time.

The acceleration for the cycler would be about 1.239E-3 meters per second per second. For the first orbit, per the orbital mechanics section, the delta V required is 10.5 kilometers per second. This leaves a burn time of 96 days, 17 hours, and 15.9 minutes using 13,195 kilograms of argon. The second and third orbit have a delta V of 11.46 kilometers per second using 14,333 kilograms of argon over 105 days. All specifications are listed in the appendix.

As an added benefit, the ion thrusters can be utilized to adjust the cycler orbit with great ease and little fuel. So, if in several decades, the cycler orbit needs to be adjusted, the entire project is not a loss and corrections can be made. This is under the assumption, though, that the engines are allowed enough time to perform the corrections.

Nuclear-Thermal Propulsion

In contrast to the ion-propulsion, the nuclear-thermal propulsion system is a much higher-thrust system with a considerably lower efficiency. The trade-off here is more fuel is used to acquire shorter burn times and stays in space. The cycler was intended for extended stays, whereas the taxi was designed primarily for short-term habitation on the order of a day or so.

This system is more commonly refereed to as a Nuclear Thermal Rocket (NTR). Hydrogen is the preferred propellant, because, for any given exhaust temperature, it results in the highest possible specific impulse, about twice that of chemical rockets. The major drawbacks to using hydrogen are that it needs to be stored cryogenically and it has a very low specific mass, even as a slush.

In selection of fuels, it must be taken into consideration that NT's require that the its coolant is initial liquid and is gaseous at the exhaust. Since there is a phase change, care must be taken to prevent this change from occurring in the reactor; this would lead to major control problems. To prevent this, we are using a reactor pressure of about 30 atmospheres.

It should also be noted that NTR's do not require a combustible fuel, but safety, available, and storage are almost always the deciding factors in fuel selection. Hydrogen was settled on because of its desirable performance qualities, availability in slush form, non-reactivity with the engine and tank materials, and for mission optimization. We will have to deal with the large volumes of fuel needed as well as contending with the fact that with a large mass fraction of hydrogen, the taxis will be essentially flying bombs should something go dreadfully wrong.

Each taxi will be equipped with two engines. One engine is sufficient for any taxi, but two provides for a good margin of safety. The engine was designed to be able to provide the necessary performance at maximum thrust to complete the taxi missions; however, running the rockets at full power all the time is not necessarily the optimal thing to do so far as maintenance and life-span are concerned.

Each engine has a reactor temperature of 1800 K, exit diameter of 2.5 meters, a pressure ratio of 500 (this is dependent on the shape of the nozzle), and uses 42.6 Kg/s at maximum thrust. For these specifications, the specific-impulse is about 836 seconds, the thrust is 349 kilonewtons, and provides an acceleration of 11.65 meters per second per

second for a 30,000 Kg wet taxi. This provides a maximum mass fraction of 3.57 or a DCX module mass of 8350 Kg. Specifications are given in the appendix.

The most fuel will be used on the approach and departure from Earth. The requirements here will be on the order of 21,000 Kg of hydrogen. On the approach to Mars, though, the fuel requirements are between 14,000 and 16,000 Kg. This allows for more mass to be moved to and from the cycler around Mars. The large mass requirements are the reasons that orbiting platforms around Earth and Mars or Phobos are necessary. The Phobos station must produce the hydrogen necessary for the taxi, and both hydrogen and oxygen for the DCX stage. In fact, the DCX stage can be unfueled until it reaches Mars orbit. Then additional mass can be loaded and used to land on Mars. The Earth station is extremely important in that the largest fuel requirements are here. Refueling cargo missions to the cycler will be necessary to keep the taxi refueled in transit. This can be done when the cycler is resupplied. Several taxi missions may be necessary for this, or a specialized tanker can be constructed for rendezvous with the cycler.

The burn times for the taxi are relatively short, less than 10 minutes, giving the astronauts feeling between 2 and 3 g-forces. Since the delta V is fixed for our approach, the mass fraction is fixed; thus, the only variables we can really adjust are the transit and burn times. Thus using smaller engines would only increase the burn time required while saving only a little on mass. Since much of the performance is dependent on the shape of the exhaust nozzle, it is necessary to design a highly efficient nozzle while trying to keep the mass as low as possible. As the pressure ratio increases, the efficiency increases with a decrease in thrust. This is not a problem because a lower thrust just means a slightly longer burn time while using less fuel and allowing for more cargo to be transported.

Conclusion

For optimum performance, the ion and NTR propulsion tandem seems to be the solution. The ion engine with the high efficiency is ideal for maneuvering a massive object like the cycler over periods of time and requires little fuel. The NTR propulsion is ideal for the taxi because of its high thrust capability. The major drawbacks to this though are the necessity of a cryogenic storage system and the large volume that the hydrogen requires. This cannot be avoided though if we wish to maintain the level of performance that is desired.

References

1. Brewer, George R., Ion Propulsion, Gorden and Breach, New York 1970

2. Griffin, Michael D., and French, James R., Space Vehicle Design, AIAA, Washington D.C., 1991

3. Hill, Philip, and Peterson, Carl, Mechanics and Thermodynamics of Propulsion, Addison-Wesley Publishing Co., Reading, Mass., 1992, pp. 651 - 684

4. Oates, Gordon C., Aerothermodynamics of Gas Turbine and Rocket Propulsion, AIAA, Washington D.C., 1988.

5. Somaras, Demetrius G., Applications of Ion Flow Dynamics, Prentice Hall, New York, 1962

6. Stuhlinger, Ernst, Ion Propulsion for Space Flight, Mc Graw Hill, New York, 1964

APPENDIX

Main Equations Used

Voltage Required

$$\Delta V = \frac{1}{2} m_i v_i^2$$

Power Required

$$P_b = \frac{Isp\ g\ T}{2\eta}$$

Exit pressure ratio

$$\frac{P_c}{P} = (1 + \frac{\gamma - 1}{2} M^2)^{\frac{\gamma}{\gamma - 1}}$$

Exit density ratio

$$\frac{\rho_c}{\rho} = (1 + \frac{\gamma - 1}{2} M^2)^{\frac{1}{\gamma - 1}}$$

Exit velocity

$$V_e = \sqrt{\frac{2\gamma}{\gamma - 1} R T_c (1 - (\frac{P_e}{P_c})^{\frac{\gamma - 1}{\gamma}}}$$

Mass flux

$$m = \rho_e V_e A_e$$

Mass flow rate

$$\tilde{m} = m\ g$$

Mass fraction of fuel

$$\frac{m_o}{m_f} = \exp(\frac{\Delta V}{g\ Isp})$$

Thrust

$$T = \dot{m} V_e$$

Specific Impulse

$$Isp = \frac{T}{\tilde{m}}$$

Cycler Propulsion

Total Mass = 130,000 Kg

Ion Propulsion

Specifications (per engine)

Fuel type	Argon
Exit Diameter	0.85 m
Efficiency	0.8
Isp	10000 s
Power Required	9,50 MW
Beam Power	7.6Mw
Potential Difference	2007.32 V
Mass flux	1,579E-3 Kg/s
Acceleration	1.239E-3 (m/s^2)
Total Thrust	154.9 N
Thrust per Engine	4.4 N
Number of engines Required	35
Safty Factor	70%
Total number of engines	60
Mass per engine	165 Kg
Total Engine Mass	9900 Kg

Orbit 1

Delta V required	10.5 Km/s
Mass fuel required	13195 Kg
Burn time	8356554.78 s
	96 days 17 hours 15.9 minutes

Orbit 2 and 3

Delta V required	11.46 Km/s
Mass fuel required	14333 Kg
Burn time	9077264.09 s
	105 days 1 hour 27.7 minutes

Taxi Propulsion

Total Mass = 30000 Kg

Nuclear Thermal Propulsion (2 engines used)

Specifications (per engine)

Fuel type	Hydrogen
Exit diameter	2.5 m
Combustion Temperature	2800 K
Combustion Pressure	30 atm
Pc/Pe	500
Mass Flow	42.6025 Kg/s
Thrust	3.49E+5 N
Isp	836.23 s
Acceleration	11.65 (m/s^2)

Orbit 1 Approach to Mars

Delta V Required	6.3152 Km/s
Mass fuel required	16108Kg
Burn time	378 s
	6.30 min.

Orbit 1 Approach to Earth

Delta V Required	9.4889 Km/s
Mass fuel required	20564.34 Kg
Burn time	482.7 s
	8.05 min.

Orbit 2 and 3 Approach to Mars

Delta V required	5.2707 Km/s
Mass Fuel Required	14220Kg
Burn time	333.78 s
	5.56 min.

Orbit 2 and 3 Approach to Earth

Delta V required	10.4554 Km/s
Mass Fuel Required	21613 Kg
Burn time	507.3 s
	8.46 min.

Maximum Mass of DCX	8386 Kg

THERMAL CONTROL

Christopher J. Robson

Overview

This section of the report summarizes the mission thermal control design objectives and results. The design process was initiated by defining a set of design objectives as follows:

- analyze and design thermal control systems to provide for the proper heat transfer between spacecraft elements so that temperature sensitive components will remain within their specified temperature limits during all mission environmental conditions
- design reliable thermal control systems utilizing proven technologies while attempting to minimize the number of moving parts and provide for adequate redundancy
- design each spacecraft component to be thermally independent of other components
- investigate both active and passive thermal control systems

Once the design objectives were determined, the critical thermal and related systems were identified as follows:

- Cryogenic Storage
- Radiation Shielding
- Nuclear Power Generation

With the design objectives in mind, various active and passive thermal control devices were employed to achieve the desired level of thermal control as described on the following pages.

I. Cryogen Storage System

The cryogenic storage system described herein is utilized for the orbital long-term storage of subcritical liquid cryogens. Although a mission of this scope would require the storage of hydrogen, oxygen, methane, argon, helium, deuterium, and nitrogen triflouride with tank sizes ranging from 0.6 m^3 to 37.4 m^3, only an analysis of the storage of those gases required by the propulsion systems follows. (14:131)

The cryogenic cooling system consists of a pressure vessel containing the saturated liquid cryogen, a structural support system, multilayer insulation ("MLI"), penetrating inflow and outflow lines, and a Molecular Absorption Cryogenic Cooler ("MACC").

Multilayer Insulation ("MLI")

Multilayer insulation consist of a number of highly reflecting radiation shields interspaced with a low thermal conductivity spacer material. The radiation shields are generally a thin Mylar or kapton film metalized on either one or both sides. Spacer materials range from very coarse silk nets to continuous materials such as borosilicate fiber sheets (i.e. tissuglas or dexiglas). (11:503) For analysis, the radiative heat transfer into spherical tanks through multilayer insulation was approximated by the radiative heat exchange between parallel plates. It was assumed that the silk net could be approximated by a noninteracting spacer. (10:477) A worst-case heat-flux of 1399 W/m^2 at 1.0 A.U. (the Cycler's closest approach to the Sun) was assumed for all calculations. As shown in Attachment #1 and Diagram #1, several combinations of materials and layers of insulation were considered before an "ideal" MLI configuration was determined.

A summary of the final MLI configuration and it's effectiveness is shown below:

Cryogenic Tank Component	Composition/Magnitude
Exterior Surface Material	Optical Solar Reflector $\varepsilon = 0.88$ $\alpha = 0.14$
Interior Surface Material	Mylar surface coated with vapor deposited 2024 aluminum $\varepsilon = 0.04$
Spacers	silk nets / tissuglas
Mylar Film Quantity & Thickness	30 layers; 270 angstrom/layer
Film/Gap Spacing	0.01 inches
Wall Thickness	0.31 inches
Rate of Heat Transfer: **liquid hydrogen (20 K)** **liquid argon (87 K)**	 **0.085 W/m²** **0.082 W/m²**
Shield Effectiveness **(reduction in overall heat transfer):** **liquid hydrogen (20 K)** **liquid argon (87 K)**	 **98.3%** **98.3%**
Comparison to Published Results: (2.3 m outer diameter hydrogen tank) calculated heat transfer rate published heat transfer rate	 0.35 W 0.48 W

Optical solar reflector was selected for the exterior surfaces of the tanks because it possesses a low α/ε ratio of 0.16 and has been shown to withstand surface degradation in the orbital radiation environment over extended periods of time. The support system for the tanks consists of low-thermal conductance high-strength tubes designed to minimize heat dissipation and provide for structural rigidity under all mission loading conditions. (14:133) Although heat transfer through the insulation normal to the layers is small, discontinuities such as seams or penetrations provide thermal "shorts" which degrade the over-all system performance. (11:503) A low conductivity ceramic standoff will be used to mount the tanks to the Cycler thus preventing conductive heating of the tanks from the warmer Cycler truss structure.

Tank/Pressure Vessel Sizing

Sizing of the cryogen tanks was performed using the calculated rate of heat transfer per unit area, a selected tank pressure of 1 atmosphere, and the mass of respective cryogen required for the mission as provided by the propulsion and design engineers. A sample calculation for this analysis is shown on Attachment #2.

In order to determine if the calculated rates of heat transfer were legitimate, the calculated results for hydrogen were compared to figures presented in Reference 15 for a design which also utilized MLI. The calculated heat transfer rate for the hydrogen tank was determined to differ from the published results by approximately 25%, which for this level of analysis seemed quite reasonable.

The overall heat transfer to the cryogen tanks, assuming the worst-case scenario as defined above, were as follows:

HYDROGEN TANKS	
Tank Diameter	5.0 m
Tank Volume	65.45 m^3
Rate of Heat Transfer	1.66 W
Mass of Hydrogen	4,647 kg

ARGON TANKS	
Tank Diameter	3.0 m
Tank Volume	14.14 m^3
Rate of Heat Transfer	0.58 W
Mass of Argon	19,655 kg

Boiloff Recondensation - Molecular Absorption Cryogenic Cooler

With the heat input as shown in the above tables, boiloff of the cryogen is inevitable. A Molecular Absorption Cryogenic Cooler ("MACC") as described in Reference 15 was selected to recondense the boiloff. Since the MACC has been used in conjunction with MLI in prior experiments, may use waste heat or direct solar heat as an energy source for the compressor, has essentially no moving parts, is compact and lightweight, has been shown to provide for the level of heat extraction required, and has never failed during testing, it is an ideal candidate for the requirements of this mission.

A summary of the MACC refrigeration cycle is shown in Attachment #3. The MACC, as described in Reference 15, operates as follows: The cooler operates by using a hydride power ($LaNi_5$) to absorb large quantities of hydrogen at temperatures around 290 K and 1 atm pressure. When heated to about 390 K, however, the hydrogen pressure increases to about 4 MPa (40 atm). The pressure from the hydrogen gas then activates a diode check valve and the hydrogen flows through a series of space radiators and heat exchangers, as shown in Attachment #3. When the gas reaches the JT valve, it is at about 30K. When expanded to 1 atm through the JT valve, it is further cooled and partially condensed. Heat from the hydrogen tank then vaporizes the condensed hydrogen, and the cycle is closed back through the counterflow heat exchangers, heating the returning hydrogen while prechilling the high-pressure hydrogen.

A summary of the MACC's specifications is shown below:

MACC Specification	Magnitude
Heat Absorption	0.48 W
MACC Mass	31 kg
Absorption to Mass Ratio	0.155 W/kg

II. Radiation Shielding

Surface Contamination and Degradation

A very important aspect of the development of thermal control surfaces is the consideration of the long duration of planned future missions. The effects of electromagnetic radiation or particle radiation on thermal control surfaces is not completely understood, but for a mission of this scope these surfaces should be space stable or have a predictable degradation values for at least 10 to 20 years. The following narrative, excerpted form Reference 8, exemplifies the need for this predictability, justifies the incorporation of secondary and redundant thermal control systems, and poses the question as to whether or not thermal control surfaces can be repaired or cleaned to remove the effects of contamination.

The α/ε ratio of the S-IVB stage of the Pegasus satellite which was coated with S-13, a paint composed of ZnO as the pigment and methyl silicone resin as the binder, was expected to start at 0.22 and increase within a year's effective lifetime of the spacecraft to not more than 0.27. The first measurements in orbit showed a value of 0.52, which increased with time in orbit. If it were not for the active thermal control provided by a louver assembly between the Pegasus electronic canister and the S-IVB, the electronics would have exceeded their thermal limits. The reason for the high values of the ratios of solar absorptance to infrared emittance was not simply the degradation caused by the space environment, but a combination of the contamination from the rocket firings and the subsequent effect of the space environment on the contaminated surfaces.

As further discussed in Reference 8 contamination of thermal control surfaces has three aspects: on the ground, during launch, and in space. Contamination on the ground occurs during assembly, thermal vacuum testing, and handling prior to and during launch. In many cases, more than a year passes between the application of coatings and the launch of a spacecraft. During launch and in space, exhaust jets from reaction control engines, which have a wide expansion cone, have been shown to produce a contamination cloud surrounding the whole space vehicle. During simulated tests in chamber A at NASA

Manned Spacecraft center contaminants from the Reaction Control System engines were found on surfaces which were behind barriers and 180° from the jets. The effect of such contamination is more serious in space because of the simultaneous effect of uv radiation. Without this irradiation the contaminants would probably leave the surface again after a short time. However, with the presence of uv radiation and the solar wind, the contaminants undergo reactions which prevent them from vaporizing and which lead to high solar absorptance.

Inflatable Solar Shields

As discussed in Reference 12, an inflatable solar shield has been developed that can be folded and packaged in a relatively small canister. Once in space the canister cover is jettisoned and the shield is deployed, inflated, and chemically rigidized over the area of the shield that is subject to high inertial loading. This provides a thermal shield that is external to the vehicle such that incident solar energy can be intercepted and then reflected and re-radiated back to space. A schematic and summary of the inflatable shield concept is presented in Attachment #4. A summary of the inflatable shield's specifications follows:

Section	Composition
Spherical Shell	3/4-mil-thick aluminum/Mylar/aluminum tri-laminate
Sun-Side	Alodine Coating (alpha = 0.3, epsilon =0.52)
Back-Side	Multiple Materials (epsilon = .90)
Foam Stiffener	open-celled foam bonded to shell; utilizing a polymerization accelerator N,N, Diethylaniline (DEA) to rigidization

The effectiveness of a solar shield is highly dependent upon the radiative properties of the shield surface. It is imperative that these properties remain relatively constant throughout the entire mission. The three coatings tested in Reference 12 were silicon oxide, alodine, and a carbon-doped polyester deposited on a substrate of the aluminum/Mylar/aluminum tri-laminate. These were selected because of their ability to maintain their surface properties after the shield is deployed and inflated from a tightly packed

configuration in its storage canister. All three materials were found to be very resistant to solar wind protons. The alodine and carbon-doped polyester coatings were also found to be very resistant to ultraviolet radiation.

Some areas of the shield require reinforcement in order to withstand inertial loads. The rigidized material developed to provide this reinforcement is a flexible open-cell polyurethane foam that is bonded to the GT-15 and them impregnated with a monomeric compound. Rigidization of the foam may be accomplished by use of a polymerization accelerator.

The effects of nuclear radiation on the properties of the rigidizable material were also investigated. Results indicate that the material will remain sufficiently flexible and that it can be successfully folded, stored, and then deployed after exposure in a vacuum at 30^0 F to an accumulated gamma dose of up to about 4×10^6 ergs/g(C).

Scale-model thermal tests indicate that the spherical solar shield is capable of maintaining backside shield temperatures between -175^0 to -200^0 F (144 - 155 K). With these characteristics, an inflatable solar shield appears to be an ideal candidate for a secondary or back-up thermal control system.

Osmotic Heat Pipes

As discussed in Reference 16, evolving future spacecraft will require a much more significant role of thermal management because of the multi-year mission duration, large quantities of waste heat to be dissipated, and long physical distances involved. Osmosis provides the capability to transport large amounts of heat over very long distances with a passive device.

A conceptual osmotic-pump-driven energy transport loop is illustrated in Attachment #4 and operates as follows: Direct osmosis is employed as the driving force that circulates working fluid inside a closed system. When two fluids of different concentrations are separated by a semipermeable membrane, the

solvent will flow into solution to attain equilibrium. The membrane is impermeable to the solute. As long as the concentration gradients are high between solvent and solvent-solute mixture (solution), flow will continue due to direct osmotic forces. The addition of heat to the solution causes solvent to evaporate and flow to the condenser, where it recondenses, giving up heat. The solvent then returns to the membrane. The passage of solvent through an osmotic membrane can create a differential pressure that is orders of magnitude greater than the capillary action created by surface tension in conventional heat-pipe wicks. Thus, osmosis provides the capability to transport large amounts of heat over very long distances with a passive device.

III. Nuclear Power Generation

Major Design Considerations

The major considerations surrounding the design and operation of a space nuclear reactor system follows:

- physics, neutronics
- fuel materials and performance
- materials for high temperature application
- control/instrumentation
- safety parameters
- high-efficiency conversion systems
- shielding and radiators (low weight)

Nuclear Reactor Power System Composition

The major subsystems contained within a nuclear reactor power system are as follows:

- **Reactor/Fuel**
- **Coolants**
  NaK mixture, hydrogen, lithium, helium, air, heat pipes
- **Shielding**

shield circumferentially surrounds core and consists of alternating layers of tungsten and lithium hydride - primarily intended to attenuate radiation directed towards the crew habitat; permits crew excursions

- **Power Conversion**
  Brayton cycle, Rankine cycle, Stirling cycle and direct conversion cycles: thermoelectric, thermionic, and magnetohydrodynamic

Candidate	Inlet Temp. (K)	Outlet Temp (K)	Thermal Efficiency
Thermoelectrics	1360	850	0.054
Rankine:			
Organic	600	400	0.20
Mercury	950	633	0.07
Potassium	1420	933	0.20
Brayton	1325	500	0.186
Stirling	1325	700	0.254
Thermionics:			
In Core	2000	910	0.10
Out of Core	1620	900	0.10

- **Heat Rejection**
  only available is heat transfer method is radiation, need high temperature rejection for efficiency, high temperature also provides for lower weight and smaller size of the radiator

This extensive list of requirements and design choices emphasizes the fact that a great deal of technical research and development effort will be required before any reactor systems is ready for use and before appropriate system/material and operational trade-offs can be made.

SP-100 Nuclear Space Power System

The SP-100 Nuclear Space Power System provides a valuable scaleable design base for this mission. The system was designed to furnish 100kWe over a seven-year lifetime. The nuclear reactor subsystem consists of a fast-spectrum $235UO_2$ fueled reactor with a liquid-metal coolant conveyed to radiators by heat pipes. (1:24)

Power conversion for the SP-100 concept is achieved using thermoelectric ("TE") converters. Thermal energy is extracted from the reactor core by heat pipes that then radiate it to panels containing thermoelectric converters. Hot shoe thermal collectors are used to concentrate this radiant energy. The

thermal energy flows through the thermoelectric material by conduction. Thermal insulation is used to minimize thermal energy losses around the thermoelectric material. Thermal energy that cannot be effectively used is then rejected to space by radiation heat transfer.

A conical-shaped radiation shield is located between the reactor and the payload. It serves as a barrier that reduces the amount of reactor-generated nuclear radiation, neutrons and gamma rays, reaching the payload sensitive portions of the spacecraft or the astronaut crew. The shield contains primarily two types of materials: low atomic weight lithium hydride (LiH) to attenuate neutrons and high atomic weight tungsten to shield against gamma radiation. (SNP:225)

Reference 3 is a study which couples the SP-100 reactor with a Brayton power conversion cycle. Of relevance for this mission is the heat rejection system utilized in the design. Waste heat from the Brayton engines is transferred to a single, gas to liquid NaK heat exchanger. The heat exchanger systems uses a shared radiator system in which the NaK is pumped through an armored manifold to a number of heat pipe radiator panels connected in series. Since this manifold is vulnerable to single point failures, an independent stand-by loop was included. (3:870) The design provides for the usage of only a portion of the radiator to reject the heat load which allow failure of a radiator panel without compromising full power output.

Another study, presented in Reference 13, tested an aluminum space radiator panel utilizing a liquid metal coolant in the 300^0 to 700^0 F temperature range. Testing of the panel in air and in vacuum confirmed its feasibility. Such a radiator would be suitable for the primary heat rejection system of a Rankine or a Brayton power cycle.

The mission's Nuclear Electric Propulsion ("NEP") reactor's requirements include:

- temperatures from 1350 to 2000 K
- firing times up to 7 years
- high fuel burnup
- power of 25 to 100 MWth (5 to 10 MWe)

The NEP system also requires also requires high temperature turbines and radiators and high temperature power conditioning. In consideration of the current state of technology and the relative success of the SP-100 Nuclear Power System, a nuclear power system for this mission was projected as follows:

Thermal Characteristics of Proposed Nuclear Power System

Component	Composition
Reactor/Fuel	undetermined
Coolant	NaK
Shielding	alternating layers of tungsten and lithium hydride
Power Conversion	**Sterling Cycle (efficiency = 0.25)**
Carnot Efficiency	**0.50**
Radiator	**1000 m² honeycomb sandwich panel heat pipe; Iconel 718 honeycomb radiator matrix & Nickel-200 cooling jacket**
Temperature Profile: Reactor Core: Converter Inlet: Radiator:	 2000 K 1600 K 1000 K

The projected reactor is envisioned to provide 10 MWe of power output. A Stirling cycle is optimal for power conversion because of its highly efficient conversion cycle (25%), its high temperature heat rejection which minimizes radiator size, its low specific mass, and its reliability. An advanced radiator design, as previously described was also selected to be used in the 1000 K temperature regime. (2:165,179)

References

1 Advanced Nuclear Systems for Portable Power in Space, Report by Committee on Advanced Nuclear Systems, Energy Engineering Board, Commission on Engineering and Technical Systems, National Academy Press, Washington D.C., 1983. pp. 13-26.

2 Angelo, J.A., and Buden D., Space Nuclear Power, Orbit Book Co. Inc., Malabar Florida, 1985. pp. 152-271

3 Mason, Rodriguez, and McKissock, "SP-100 Reactor with Brayton Cycle Conversion for Lunar Surface Applications," Conference 920104, American Institute of Physics, NASA Lewis Research Center Publication, 1992.

4 Selcow, Davis, Perkins, Ludewig, and Cerbone, "Assessment of the use of H_2, CH_4, NH_3, and CO_2 as NTR Propellants," Conference 920104, American Institute of Physics, Brookhaven National Laboratory Publication, 1992.

5 Clark, John S., "The NASA/DOE Space Nuclear Propulsion Project Plan - FY 1991 Status," Conference 920104, American Institute of Physics, NASA Lewis Research Center Publication, 1992.

6 Lazareth, Schmidt, Ludewig, and Powell, "Human Round Trip to Mars: Six Months and Radiation Safe," Conference 920104, American Institute of Physics, Brookhaven National Laboratory Publication, 1992.

7 Agrawal, B.N., Design of Geosynchronous Spacecraft, Prentice-Hall, Englewood Cliffs, NJ, 1986.

8 "The Status of Thermophysics as a Multidiscipline Area in Astronautics and Aeronautics ," Progress in Astronautics and Aeronautics: Volume 24: Heat Transfer and Spacecraft Thermal Control, Lucas, J.W. Wd., Alpine Press, Inc., 1971.

9 "Effects of Ultraviolet Irradiation on Zinc Oxide ," Progress in Astronautics and Aeronautics: Volume 24: Heat Transfer and Spacecraft Thermal Control, Lucas, J.W. Wd., Alpine Press, Inc., 1971.

10 "Effective Conductance Along Parallel Radiation Shields," Progress in Astronautics and Aeronautics: Volume 24: Heat Transfer and Spacecraft Thermal Control, Lucas, J.W. Wd., Alpine Press, Inc., 1971.

11 "Numerical Evaluation of Multilayer Insulation System Performance," Progress in Astronautics and Aeronautics: Volume 24: Heat Transfer and Spacecraft Thermal Control, Lucas, J.W. Wd., Alpine Press, Inc., 1971.

12 "Thermal Testing of Inflatable Solar Shields for Cryogenic Space Vehicles," Progress in Astronautics and Aeronautics: Volume 24: Heat Transfer and Spacecraft Thermal Control, Lucas, J.W. Wd., Alpine Press, Inc., 1971

13 "Testing of an Aluminum Radiator with Liquid Metal Coolant," Progress in Astronautics and Aeronautics: Volume 24: Heat Transfer and Spacecraft Thermal Control, Lucas, J.W. Wd., Alpine Press, Inc., 1971

14 "Thermodynamic Optimization of a Cryogenic Storage System for Minimum Boiloff," Progress in Astronautics and Aeronautics: Volume 86: Spacecraft Thermal Control, Design, and Operation, Collicott and Bauer, AIAA, 1983.

15 "Molecular Absorption Cryogenic Cooler for Liquid Hydrogen Propulsion Systems," Progress in Astronautics and Aeronautics: Volume 86: Spacecraft Thermal Control, Design, and Operation, Collicott and Bauer, AIAA, 1983.

16 "Osmotic Pumped Heat Pipes for Large Space Platforms," Progress in Astronautics and Aeronautics: Volume 86: Spacecraft Thermal Control, Design, and Operation, Collicott and Bauer, AIAA, 1983.

17 Holman, J.P., Heat Transfer, Seventh Edition, McGraw-Hill Publishing Company., 1990.

18 Meyer, R.X., "Notes for MANE 161B: Introduction to Space Technology," University of California, Los Angeles.

CRYOGENIC STORAGE SYSTEM

Multilayer Insulation

Requirements:
- solar radiation flux at 1.0 A.U.
- explore several possibilities

Approximations:
- radiative exchange between parallel plates
- noninteracting spacers (silk net/tissuglas)

CASE	exterior surface	interior surface	
A	aluminized kapton	6061 aluminum	
B	tiodized titanium	6061 aluminum	
C	white silcone paint	6061 aluminum	(cool)
D	gold plate	6061 aluminum	(hot)
*E	optical solar reflector	2024 aluminum	

	CASE A	CASE B	CASE C	CASE D	CASE E
Solar Flux, Is (W/m^2) =	1399	1399	1399	1399	1399
exterior surface, epsilon:	0.6	0.6	0.88	0.043	0.88
exterior surface, alpha:	0.5	0.6	0.14	0.215	0.14
ext. alpha/epsilon =	0.83	1.00	0.16	5.00	0.16
interior surfaces, epsilon:	0.07	0.07	0.07	0.07	0.05
insulation, epsilon:	0.07	0.07	0.07	0.07	0.05
Boltzmann constant (W/(m^2*K^4):	5.70E-08	5.70E-08	5.70E-08	5.70E-08	5.70E-08
Temp of Outer Surface, To (K) =	361.3	378.2	217.0	1093.0	217.0
Temperature of Inner Surface, Ti =	20	20	20	20	20
Case I - No Shield Used					
total resistance =	14.95	14.95	14.42	36.54	20.14
total heat transfer, q/A (W/m^2) =	64.97	77.97	8.77	2225.88	6.28
Case II - One Shield Used					
total resistance =	42.52	42.52	41.99	64.11	59.14
total heat transfer, q/A (W/m^2) =	22.85	27.42	3.01	1268.65	2.14
Case III - Two Shields Used					
total resistance =	70.10	70.10	69.56	91.68	98.14
total heat transfer, q/A (W/m^2) =	13.86	16.63	1.82	887.14	1.29
Case IV - Three Shields Used					
total resistance =	97.67	97.67	97.14	119.26	137.14
total heat transfer, q/A (W/m^2) =	9.95	11.94	1.30	682.04	0.92
Case V - 100 Shields Used					
total resistance =	2772.10	2772.10	2771.56	2793.68	3920.14
total heat transfer, q/A (W/m^2) =	0.35	0.42	0.05	29.11	0.03

Scaling Notes:

Aluminum film thickness:	270 angstrom
Gap Spacing:	0.01 inches
Packing Density:	97.6 layers/inch

CRYOGENIC STORAGE SYSTEM

Multilayer Insulation

Assumptions
- solar radiation flux at 1.0 A.U.
- radiative exchange between parallel plates
- noninteracting spacers (silk net/tissuglas)

Exterior Surface : optical solar reflector
Interior Surface: 2024 aluminum

	LIQUID HYDROGEN	LIQUID ARGON
Solar Flux, Is (W/m^2) =	1399	1399
exterior surface, epsilon:	0.88	0.88
exterior surface, alpha:	0.14	0.14
ext. alpha/epsilon =	0.16	0.16
interior surfaces, epsilon:	0.04	0.04
insulation, epsilon:	0.04	0.04
Boltzmann constant (W/(m^2*K^4):	5.70E-08	5.70E-08
Temp of Outer Surface, To (K) =	**217.0**	**217.0**
Temperature of Inner Surface, Ti =	**20.26**	**87.29**
No Shield Used		
total resistance =	25.14	25.14
total heat transfer, q/A (W/m^2) =	5.03	4.90
30 Shields Used		
total resistance =	**1495.14**	**1495.14**
total heat transfer, q/A (W/m^2) =	**0.0845740**	**0.0823674**
% Reduction in Heat Flux =	**-98.32%**	**-98.32%**

Scaling Notes:

Aluminum film thickness:	270	angstrom
Gap Spacing:	0.01	inches
Packing Density:	97.6	layers/inch
Wall thickness for 30 Shields:	**0.31**	**inches**

FIGURE #1

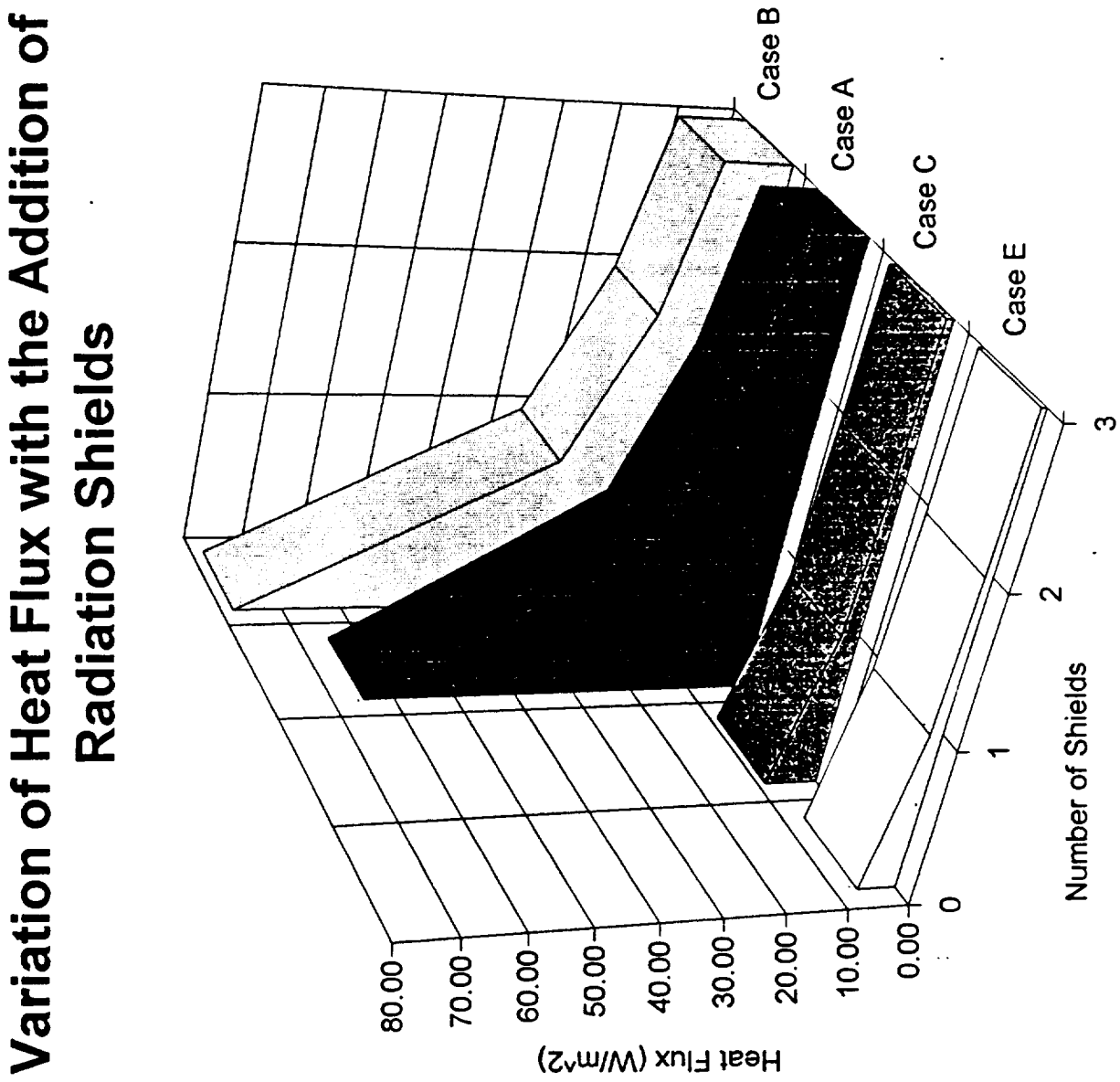
Variation of Heat Flux with the Addition of Radiation Shields
Case B
Case A
Case C
Case E
80.00
70.00
60.00
50.00
40.00
30.00
20.00
10.00
0.00
Heat Flux (W/m^2)
0
1
2
3
Number of Shields

CRYOGENIC STORAGE SYSTEM

Tank Sizing Analysis

			LIQUID HYDROGEN		LIQUID ARGON	
			q/A (W/m^2)=	0.084574	q/A (W/m^2)=	0.0823674
Radius (m)	Volume (m^3)	Effective Area (m^2)	Heat Tansfer Rate (W - J/s)	H.T.R. per Unit Volume	Heat Tansfer Rate (W - J/s)	H.T.R. per Unit Volume
1.0	4.19	3.14	0.27	0.0634	0.26	0.0618
1.5	**14.14**	**7.07**	**0.60**	**0.0423**	**0.58**	**0.0412**
2.5	**65.45**	**19.63**	**1.66**	**0.0254**	**1.62**	**0.0247**
4.0	268.08	50.27	4.25	0.0159	4.14	0.0154
5.0	523.60	78.54	6.64	0.0127	6.47	0.0124
6.0	904.78	113.10	9.57	0.0106	9.32	0.0103
7.0	1,436.75	153.94	13.02	0.0091	12.68	0.0088
8.0	2,144.66	201.06	17.00	0.0079	16.56	0.0077
9.0	3,053.63	254.47	21.52	0.0070	20.96	0.0069
10.0	4,188.79	314.16	26.57	0.0063	25.88	0.0062
11.0	5,575.28	380.13	32.15	0.0058	31.31	0.0056
12.0	7,238.22	452.39	38.26	0.0053	37.26	0.0051
13.0	9,202.76	530.93	44.90	0.0049	43.73	0.0048
14.0	11,494.03	615.75	52.08	0.0045	50.72	0.0044
15.0	14,137.16	706.86	59.78	0.0042	58.22	0.0041

Boiloff Rate Determination

Assumptions:
- thickness of tank wall can be ignored

	LIQUID HYDROGEN		LIQUID ARGON	
Heat Transfer Rate:	**1.66E-03**	**kJ/s**	**5.82E-04**	**kJ/s**
Enthalpy of Vaporization:	**446.42**	**kJ/kg**	**163.29**	**kJ/kg**
Rate of Boiloff:	**3.72E-06**	**kg/s**	**3.57E-06**	**kg/s**
Density @ Boiling Point:	**71.0**	**kg/m^3**	**1390.0**	**kg/m^3**
Mass of Tank Contents:	**1,004**	**kg**	**19,651**	**kg**
% Mass Boiloff Per Day:	**0.0320%**		**0.0016%**	

CRYOGENIC STORAGE SYSTEM

BOIL-OFF RECONDENSATIOi! ANALYSIS

Assumptions:
Ideal Cycle: Reversed Carnot thermodynamic cycle (refrigeration cycle)
Composed of four reversible processes:
- (1-2) reversible isothermal expansion
- (2-3) reversible adiabatic expansion
- (3-4) reversible isothermal compression
- (4-5) reversible adiabatic expansion

Yields maximum possible efficiency between two reserviors

Radiator Surface Temperature (Th) =	**250 K**

HYDROGEN

Heat Transfer Rate =	**1.66E-03 kJ/s**
Inner Surface Hydrogen (T hy,low) =	**20.26 K**
Thermal Efficiency, nth,rev =	**0.92**
Efficiency @ 70% Carnot =	**0.64**
Efficiency @ 30% Carnot =	**0.28**
COP =	**0.0882**
Work Input/Power Required =	**1.88E-02 kJ/s**

ARGON

Heat Transfer Rate =	**5.82E-04 kJ/s**
Inner Surface Argon (T ar,low) =	**87.29 K**
Thermal Efficiency, nth,rev =	**0.65**
Efficiency @ 70% Carnot =	**0.46**
Efficiency @ 30% Carnot =	**0.20**
COP =	**0.5365**
Work Input/Power Required =	**1.08E-03 kJ/s**

FLAT-PLATE RADIATOR SIZING

Assumptions:
- flat plate radiator
- set at incidence angle of 90 degrees(edge on) to incoming solar flux a 1.0 A.U.
- area requirement set by fixed temperature of the sink
- surface: optical solar reflector (alpha = 0.14, epsilon = 0.88)

HYDROGEN

Heat Transfer Rate =	**1.66 J/s**
Required Area =	**0.0042 m^2**

ARGON

Heat Transfer Rate =	**0.58 J/s**
	0.0015 m^2

CRYOGENIC COOLING SYSTEM DESIGN

BOIL-OFF RECONDENSATION
MOLECULAR ABSORPTION CRYOGENIC COOLER ("MACC")

MACC Characteristic	Magnitude
Mass	31 kg
Heat Absorption	0.48 W
Absorption to Weight Ratio	0.155 W/kg

- used in conjunction with MLI configuration
- essentially no moving parts
- hydrogen working fluid
- long-life; no mechanical failure during any test periods

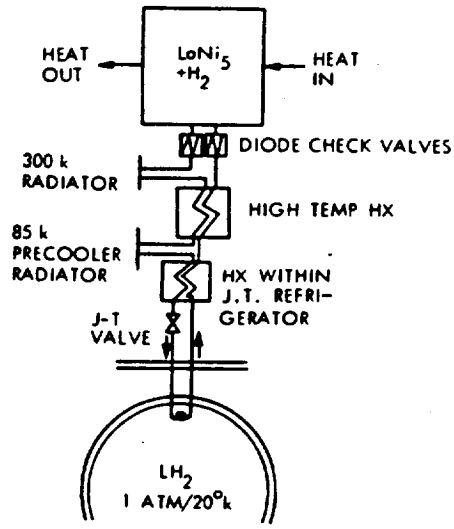

REFRIGERATION CYCLE
(continuous flow - pressure)

"COMPRESSOR" (1-2)	i) hydride power ($LaNi_5$) used to absorb large quantities of hydrogen at T = 290 K, P = 1 atm
"CONDENSER" (2-3)	ii) heat hydrogen to 390 K, P increases to 4 MPa (40 atm) iii) pressure activates diode check value and hydrogen flows through a series of space radiators and heat exchangers
"EXPANSION-THROTTLING" (3-4)	iv) at the JT valve T = 30 K; hydrogen is expanded to 1 atm and is further cooled and condensed
"EVAPORATOR" (4-1)	v) enter hydrogen tank; heat from hydrogen fuel tank vaporizes the condensed hydrogen vi) cycle is closed back through the counterflow heat exchangers heating the hydrogen and prechilling the high-pressure hydrogen

OSMOTIC HEAT PIPE

- **allows for the passive transport of heat over large distances**
- driving force is osmosis - two fluids of different concentrations separated by a semipermeable membrane; the solvent will flow into solution to gain equilibrium; membrane is impermeable to the solute
- pumping force proportional to the concentration gradient

1. Heat addition to the solution causes solvent to evaporate and flow to the condenser, where it recondenses, giving up heat
2. Solvent returns to membrane
3. Passes through an osmotic membrane, creating a differential pressure that is orders of magnitude greater than the capillary action created by surface tension in conventional heat pipe wicks.

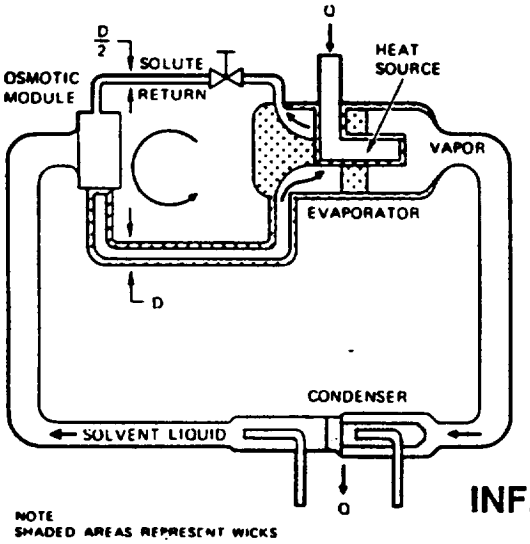

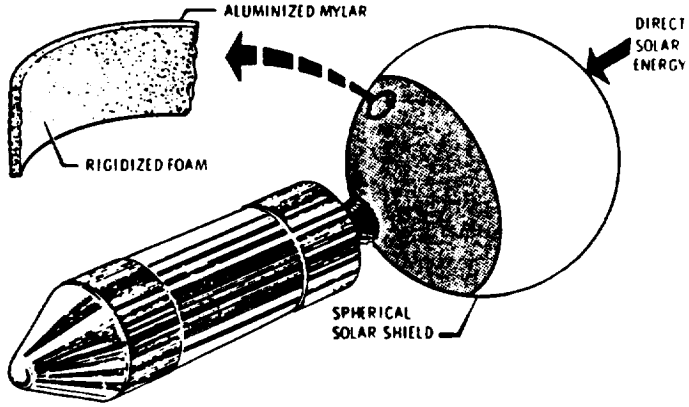

INFLATABLE SHIELDS

- packaged in a canister; once in space the canister cover is jettisoned and the shield is deployed, inflated, and chemically rigidized
- provides a thermal shield that is external to the vehicle such that incident solar radiation can be intercepted and then reflected and re-radiated back to space
- reduces the need for active thermal control devices
- system can withstand gamma doses of up to 4 X 10^6 ergs/g (C) at 30° F without undergoing premature polymerization

Section	Composition
Spherical Shell	3/4-mil-thick aluminum/mylar/aluminum tri-laminate
Sun-Side	Alodine Coating (alpha = 0.3, epsilon =0.52)
Back-Side	Multiple Materials (epsilon = .90)
Foam Stiffener	open-celled foam bonded to shell; utilizing a polymerization accelerator N,N, Diethylaniline (DEA) to rigidization

EFFECTIVENESS: Backside shield temperatures between 144-155 K.

MANE 161C
MANNED MISSION TO MARS

ATTACHMENT #5

SUMMARY OF THERMAL CONTROL ANALYSIS

DESIGN OBJECTIVES:

- analyze and design thermal control systems to provide for the proper heat transfer between spacecraft elements so that temperature sensitive components will remain within their specified temperature limits during all mission environmental conditions
- design reliable and redundant systems utilizing proven technologies and minimal numbers of moving parts
- design each spacecraft component to be thermally independent of the system
- investigate both active and passive thermal control systems

DESIGN RESULTS:

☑ Cryogenic Cooling System - Multilayer Insulation

Component	Composition/Magnitude
Exterior Surface Material	Optical Solar Reflector
Interior Surface Material	mylar - vapor deposited 2024 aluminum
Spacers	Silk Net / Tissuglass
Film Thickness	270 angstrom
Gap Spacing	0.01 inches
Wall Thickness	0.31 inches
Rate of Heat Transfer: liquid hydrogen (20 K) liquid argon (87 K)	 0.0846 W/m^2 0.0824 W/m^2
Shield Effectiveness: liquid hydrogen (20 K) liquid argon (87 K)	 98.32% 98.32%
Comparison to Published Results: (2.3 m OD hydrogen tank) calculated heat transfer rate published heat transfer rate	 0.35 W 0.48 W

☑ Cyrogenic Cooling System - Boiloff Recondensation

Utilization of **Molecular Absorption Cryogenic Cooler ("MACC")**

Component	Composition/Magnitude
Heat Absorption	0.48 W
MACC Mass	31 kg
Absorption to Mass Ratio	0.155 W/kg

- compact; essentially no moving parts; reliable - no mechanical failures during testing

☑ Alternative Thermal Control Techniques (Active & Passive)

⇨Thermal Coatings & Insulation (Degradation/Contamination)
⇨Osmotic Heat Pipe
⇨Inflatable Shields
⇨Louvers
⇨Electrical Heaters

☑ Space Nuclear Power

Nuclear Reactor Power System Composition:

- **Reactor/Fuel:** uranium carbide, uranium nitride, and uranium oxide
- **Coolants:** Na, NaK mixture, hydrogen, lithium, helium, air, heat pipes
- **Shielding:** shield circumferentially surrounds core and consists of alternating layers of tungsten and lithium hydride - primarily intended to attenuate radiation directed towards the crew habitat
- **Power Conversion:** Brayton cycle, Rankine cycle, Sterling cycle and direct conversion cycles: thermoelectric, thermionic, and magnetohydrodynamic
- **Heat Rejection:** only available is heat transfer method is radiation, need high temperature rejection for efficiency, high temperature also provides for lower weight and smaller size of the radiator

State of Technology:

- components for system have been identified; several reactor types, fuel elements, and coolants are available
- an "optimized" system has not been designed
- technology is not in hand for a manned Mars mission

Proposed Nuclear Power System

Component	Composition
Reactor/Fuel	undetermined
Coolant	NaK
Shielding	alternating layers of tungsten and lithium hydride
Power Conversion	Sterling Cycle
Radiator	honeycomb sandwich panel heat pipe; Iconel 718 honeycomb radiator matrix & Nickel-200 cooling jacket
Temperature Profile: Reactor Core: Converter Inlet: Radiator Reject:	 2000 K 1600 K 1000 K

Conclusion: A great deal of technical research and developments effort will be required before any reactor system is ready for use and before appropriate system/material and operational trade-offs can be made.